Molecular Biology of the Cell
Vol. 18, 4420–4437, November 2007

ARL4D Recruits Cytohesin-2/ARNO to Modulate Actin Remodeling[D]

Chun-Chun Li,* Tsai-Chen Chiang,* Tsung-Sheng Wu,* Gustavo Pacheco-Rodriguez,† Joel Moss,† and Fang-Jen S. Lee*

*Institute of Molecular Medicine, College of Medicine, National Taiwan University, and Department of Medical Research, National Taiwan University Hospital, Taipei 100, Taiwan; and †Pulmonary-Critical Care Medicine Branch, National Heart, Lung, and Blood Institute, National Institutes of Health, Bethesda, MD 20892-1434

Submitted February 20, 2007; Revised August 21, 2007; Accepted August 27, 2007
Monitoring Editor: Francis Barr

ARL4D is a developmentally regulated member of the ADP-ribosylation factor/ARF-like protein (ARF/ARL) family of Ras-related GTPases. Although the primary structure of ARL4D is very similar to that of other ARF/ARL molecules, its function remains unclear. Cytohesin-2/ARF nucleotide-binding-site opener (ARNO) is a guanine nucleotide-exchange factor (GEF) for ARF, and, at the plasma membrane, it can activate ARF6 to regulate actin reorganization and membrane ruffling. We show here that ARL4D interacts with the C-terminal pleckstrin homology (PH) and polybasic c domains of cytohesin-2/ARNO in a GTP-dependent manner. Localization of ARL4D at the plasma membrane is GTP- and N-terminal myristoylation-dependent. ARL4D(Q80L), a putative active form of ARL4D, induced accumulation of cytohesin-2/ARNO at the plasma membrane. Consistent with a known action of cytohesin-2/ARNO, ARL4D(Q80L) increased GTP-bound ARF6 and induced disassembly of actin stress fibers. Expression of inactive cytohesin-2/ARNO(E156K) or small interfering RNA knockdown of cytohesin-2/ARNO blocked ARL4D-mediated disassembly of actin stress fibers. Similar to the results with cytohesin-2/ARNO or ARF6, reduction of ARL4D suppressed cell migration activity. Furthermore, ARL4D-induced translocation of cytohesin-2/ARNO did not require phosphoinositide 3-kinase activation. Together, these data demonstrate that ARL4D acts as a novel upstream regulator of cytohesin-2/ARNO to promote ARF6 activation and modulate actin remodeling.

INTRODUCTION

ADP-ribosylation factors (ARFs) are small GTPases involved in membrane transport, maintenance of organelle integrity, and activation of phospholipase D and phosphatidylinositol 4-phosphate 5-kinase (Moss and Vaughan, 1998; Chavrier and Goud, 1999; Takai *et al*., 2001; D'Souza-Schorey and Chavrier, 2006). ARF1 is mainly associated with the Golgi apparatus, and it regulates vesicle budding of transport events (Stearns *et al*., 1990; Balch *et al*., 1992). ARF6 can regulate peripheral membrane dynamics and actin rearrangements at the plasma membrane (Donaldson, 2003; Sabe, 2003) such as stress fibers disassembly (D'Souza-Schorey *et al*., 1997; Boshans *et al*., 2000), formation of plasma membrane protrusions and ruffles (Radhakrishna *et al*., 1996; D'Souza-Schorey *et al*., 1997; Franco *et al*., 1999), cell migration (Palacios *et al*., 2001; Santy and Casanova, 2001), cell adhesion (Palacios *et al*., 2001), and regulation of endosomal membrane traffic (D'Souza-Schorey *et al*., 1995; Radhakrishna and Donaldson, 1997). Similar to other guanosine triphosphate (GTP)-binding proteins, ARF function depends on the highly controlled binding and hydrolysis of GTP. The conformational changes that accompany the binding of GDP or GTP can lead directly to changes in the affinity of the GTPase for proteins, lipids, and membranes. Interconversion between the two states of ARFs is most likely achieved through guanine nucleotide-exchange factors (GEFs) and GTPase-activating proteins (GAPs) (Moss and Vaughan, 1998; Donaldson and Jackson, 2000; Jackson and Casanova, 2000).

ARF-GEFs are linked to vesicular trafficking and cytoskeletal events underlying cell movement, secretion, and endocytosis (Jackson *et al*., 2000; Shin and Nakayama, 2004). ARF-GEFs that have homology with the Sec7 domain of yeast Sec7p have been identified by their ability to catalyze the exchange of GDP for GTP on ARF proteins in vitro (Chardin *et al*., 1996; Jackson and Casanova, 2000); the Sec7 domain is the only region of significant sequence similarity among ARF-GEFs, and the Sec7 domain alone is sufficient for guanine nucleotide-exchange activity (Chardin *et al*., 1996; Beraud-Dufour *et al*., 1998; Cherfils *et al*., 1998; Mossessova *et al*., 1998; Kremer *et al*., 2004). To date, four members of cytohesin ARF-GEFs that are >77% identical have been identified, including cytohesin-1, cytohesin-2/ARF nucleotide-binding-site opener (ARNO), cytohesin-3/general

This article was published online ahead of print in *MBC in Press* (http://www.molbiolcell.org/cgi/doi/10.1091/mbc.E07–02–0149) on September 5, 2007.

[D] The online version of this article contains supplemental material at *MBC Online* (http://www.molbiolcell.org).

Address correspondence to: Fang-Jen S. Lee (fangjen@ha.mc.ntu.edu.tw).

Abbreviations used: AD, activation domain; ARF, ADP-ribosylation factor; ARL, ARF-like protein; ARNO, ARF nucleotide-binding-site opener; BD, binding domain; GAP, GTPase-activating protein; GEF, guanine nucleotide-exchange factor; GST, glutathione *S*-transferase; NLS, nuclear localization signal; PAGE, polyacrylamide gel electrophoresis; PBS, phosphate-buffered saline; PCR, polymerase chain reaction; PH, pleckstrin homology; PI3K, phosphoinositide 3-kinase; PIP_3, phosphatidylinositol 3,4,5-trisphosphate; TBS, Tris-buffered saline; GRP1, general receptor for phosphoinositides 1.

receptor for phosphoinositides 1, and cytohesin-4. This family is characterized by a molecular structure that consists of an N-terminal coiled-coil domain, a central Sec7 domain, followed by a pleckstrin homology (PH) domain and an adjacent carboxy-terminal polybasic c domain (Nagel *et al*., 1998a; Santy *et al*., 1999; Jackson and Casanova, 2000; Ogasawara *et al*., 2000; Dierks *et al*., 2001). The coiled-coil domain of the cytohesin proteins mediates homodimerization and also participates in protein–protein interaction. PH domains of cytohesins bind the lipid second messengers phosphatidylinositol 3,4,5-trisphosphate (PIP_3) or phosphatidylinositol bisphosphate in vitro. The cytohesins seem to be involved in ARF6-mediated membrane trafficking and cytoskeletal reorganization (Jackson *et al*., 2000; Dierks *et al*., 2001; Santy and Casanova, 2001; Moss and Vaughan, 2002). In cells stimulated with an appropriate agonist, cytohesins can translocate from cytosol to plasma membrane to activate ARF6 in a phosphoinositide 3-kinase (PI3K)-dependent manner that requires both the PH and Sec7 domains of the cytohesin (Hemmings, 1997; Nagel *et al*., 1998b; Venkateswarlu *et al*., 1998; Venkateswarlu *et al*., 1999; Cullen and Chardin, 2000; Venkateswarlu, 2003).

ARLs share 40–60% amino acid sequence identity with ARFs and are highly conserved throughout eukaryotic evolution (Burd *et al*., 2004; Kahn *et al*., 2006). The best-characterized ARL protein, ARL1 is localized to the *trans*-Golgi network (TGN) and regulates trafficking in the TGN-endosomal pathways (Lu *et al*., 2004). ARL2 regulates the folding of β-tubulin (Bhamidipati *et al*., 2000). ARL4A, ARL4C, and ARL4D, whose expression is differentiation dependent, developmentally regulated, and tissue specific, may function in the nucleus (Schurmann *et al*., 1994; Jacobs *et al*., 1999; Lin *et al*., 2000, 2002). Disruption of the ARL4A gene in mice can reduce sperm count and a role(s) for ARL4A in the early stages of spermatogenesis in adults is inferred (Schurmann *et al*., 2002). ARL4D was identified as an open-reading frame in a genomic region containing the BRCA1 gene (Harshman *et al*., 1995; Smith *et al*., 1995) and was reported to interact with HP1 (Lin *et al*., 2002). Nevertheless, until now, relatively little is known about the cellular functions of ARL4D. To obtain additional clues to its physiological role(s), we attempted to identify interacting proteins, which may be downstream effectors.

Here, we present evidence that the ARF6-GEF, ARNO, is an effector of ARL4D. ARL4D interacted with ARNO in a GTP-dependent manner and the interaction required the C-terminal PH and polybasic c domains of ARNO. Localization of ARL4D to the plasma membrane was GTP dependent but it was not altered in ARNO knockdown cells or those overexpressing ARNO(E156K). In addition, ARL4D induced translocation of ARNO to the plasma membrane, with activation of ARF6 and loss of actin stress fibers. Knockdown of ARNO suppressed the effect of activated ARL4D on actin remodeling. ARL4D-induced redistribution of ARNO to the plasma membrane was not dependent on PI3K activation. These findings demonstrate a key role for ARL4D in the recruitment of cytohesin-2/ARNO to the plasma membrane along with ARF6 activation and actin remodeling.

MATERIALS AND METHODS

Antibodies

ARL4D antibodies were raised by immunizing rabbits with peptide N or peptide B corresponding to amino acids (a.a.) 2-18 (GNHLTEMAPTASSFLPC) or a.a. 139-155 (QPGALSAAEVEKRLAVR) of ARL4D, respectively. Rabbit anti-myc and FLAG antibodies were generated against the epitope tags, and a calnexin antibody was prepared against a peptide DTSAPTSPKVTYKAPVPSGC corresponding to a.a. 50-68 of calnexin. Other monoclonal antibodies used were myc 9E10 (BAbCO, Richmond, CA), FLAG M2, α-tubulin, ARNO (Sigma-Aldrich, St. Louis, MO), ARF6, Na^+/K^+ ATPase (Santa Cruz Biotechnology, Santa Cruz, CA), Akt, phospho-Akt (Ser473) (Cell Signaling Technology, Danvers, MA), and plasma membrane calcium pump pan ATPase (PMCA) (Abcam, Cambridge, MA). Horseradish peroxidase-conjugated sheep anti-rabbit or anti-mouse immunoglobulin (IgG) antibodies were from GE Healthcare (Little Chalfont, Buckinghamshire, United Kingdom). Alexa Fluor 594, 488, or 350-conjugated anti-rabbit and anti-mouse antibodies were purchased from Invitrogen (Carlsbad, CA).

Expression Plasmids

ARL4D and mutants (Lin *et al*., 2002) were subcloned into the mammalian expression vector pSG5 (Stratagene, La Jolla, CA). For expression as fusion with the LexA DNA-binding domain (BD) in yeast, the cDNA fragments of ARL4D and other ARF/ARLs cloned into the pBTM116 plasmid were used as described previously (Lin *et al*., 2002). ARNO and its deletion mutant cDNA sequences were amplified by polymerase chain reaction (PCR) by using ARNO/pACT2 plasmid as a template (obtained from yeast two-hybrid screen) and oligonucleotide primers incorporating restriction sites. To introduce site-specific mutations in ARNO, a two-step recombinant PCR procedure was used. To generate ARNOC7A, seven basic charge amino acids in the polybasic c domain were replaced with alanine ($_{386}$RKKRISVKKKQEQP399→$_{386}$AAAAISVAAAQEQP399), by using a 3′ primer in which the basic residues were replaced by alanine codons (5′ CTC GAG TCA GGG CTG CTC CTG TGC TGC TGC GAC TGA AAT TGC TGC TGC TGC CGC TGC CAG CAT CTC ATA 3′). These constructs were subcloned in pACT2 for yeast two-hybrid assay. For expression as GST-fusion protein in *Escherichia coli* and N-terminal FLAG-fusion protein in mammalian cells, ARNO was cloned into pGEX-4T (GE Healthcare) and pCMV-Tag2 (Stratagene) vectors, respectively. For production of recombinant His-tagged proteins, ARNO and ARNO(E156K) were subcloned into the bacterial expression vector pET15b (Novagen, Madison, WI). ARF6 and ARL4D were cloned into the expression vector pET43a (Novagen). pACYC177/ET3d/yNMT, which encodes yeast (*Saccharomyces cerevisiae*) *N*-myristoyltransferase (Lin *et al*., 2002) was used to myristoylate ARF6 and ARL4D in *Escherichia coli*. Cytohesin-3 and cytohesin-4 cDNA were synthesized by PCR from a prostatic adenocarcinoma cDNA pool (Clontech, Mountain View, CA), respectively. The GGA3 cDNA was amplified from a HeLa cell cDNA pool. Cytohesin-1 cDNA was kindly provided by Dr. M. Vaughan (National Institutes of Health, Bethesda, MD). Plasmid expressing Akt-PH-green fluorescent protein (GFP), which contains AKT1 (a.a. 1-164) with the PH domain (a.a. 6-107), was obtained from Dr. Z.-F. Chang (National Taiwan University, Taipei, Taiwan). Sequences of all constructs were confirmed by double-stranded sequencing.

Yeast Two-Hybrid Screen and Interaction Assay

The yeast strain L40 was constructed with two readouts for an interaction of histidine auxotrophy and β-galactosidase expression with the use of the LexA DNA-binding domain and GAL4-activation domain system. Using a lithium acetate transformation protocol (Clontech), mouse embryonic day 7 pACT2 cDNA library (Clontech) was screened using ARL4D(Q80L) as bait. The yeast two-hybrid screen and interaction assay was performed essentially as described previously (Lin *et al*., 2000, 2002). For histidine auxotrophy and β-galactosidase expression, we screened 6×10^6 clones, and we obtained 73 clones that specifically interacted with ARL4D(Q80L).

Guanosine 5′-O-(3-thio)triphosphate (GTPγS) Binding Assay

Preparation and purification of recombinant proteins were carried out as described previously (Pacheco-Rodriguez *et al*., 1998; Lin *et al*., 2000) The GTPγS-binding assay was carried out in a rapid filtration system as described previously (Pacheco-Rodriguez *et al*., 1998; Lin *et al*., 2000; Ogasawara *et al*., 2000) with minor modification. Briefly, 50 μl of the reaction buffer (20 mM Tris-HCl, pH 8.0, 50 mM NaCl, 1 mM EDTA, 1 mM NaN_3, 250 mM sucrose, 2 mM $MgCl_2$, and 2 mM dithiothreitol [DTT]) containing 1 μg (~1 μM) of ARF6 or ARL4D; 40 μg of bovine serum albumin; 10 μg of L-α-phosphatidyl-L-serine; 0.1 μg each of aprotinin, leupeptin, and soybean, and lima bean trypsin inhibitors; 0.5 mM 4-(2-aminoethyl) benzenesulfonyl fluoride hydrochloride; ARNO or ARNO(E156K) (1 μg unless otherwise specified); and 4 μM [^{35}S]GTPγS (~2×10^6 cpm) were incubated for the indicated time at 30°C. The exchange reaction was terminated by cooling the sample on ice and transferring to nitrocellulose filters followed by washing six times with 2 ml of ice-cold wash buffer (25 mM Tris-HCl, pH 8.0, 5 mM $MgCl_2$, 100 mM NaCl, 1 mM DTT, and 1 mM EDTA). Scintillation fluid was added to the filters, and they were counted in an LS 5000 beta-counter (Beckman Coulter, Fullerton, CA) to quantify the amount of [^{35}S]GTPγS-bound protein. Data are reported as means ± SD of values from triplicate assays in a representative experiment. All observations have been replicated at least twice with different preparations of recombinant proteins.

SDS-Polyacrylamide Gel Electrophoresis (PAGE) and Immunoblotting Analysis

SDS-PAGE was performed according to the method of Laemmli (1970). Protein was visualized by Coomassie Brilliant Blue stain. For immunoblotting analysis, proteins were separated on SDS gel and electrotransferred to polyvinylidene difluoride membranes (Millipore, Billerica, MA). Blocking and

antibody dilutions were made in 5% low-fat dry milk in Tris-buffered saline (TBS) containing 0.1% Tween 20. Washing steps were in TBS containing 0.1% Tween 20. Membranes were blocked overnight at 4°C; primary and secondary antibodies were each incubated for 1 h at room temperature. Blots were developed using secondary antibodies coupled to horseradish peroxidase (GE Healthcare), and the immunoreactive bands were detected using the ECL system (GE Healthcare) after exposure to x-ray film. In peptide competition experiments, ~30 μg of cell was loaded for each lane. The diluted primary antibody solution was preincubated overnight with equal amounts of immunogen (immunized peptide dissolved in dimethyl sulfoxide [DMSO]) or a control peptide.

Cell Culture and Transfection

COS-7 and human embryonic kidney (HEK) 293T cells were maintained in DMEM (Hyclone Laboratories, Logan, UT), supplemented with 10% fetal bovine serum (FBS) (Hyclone Laboratories), 100 U/ml penicillin, and 100 μg/ml streptomycin (Invitrogen) in a humidified incubator with 5% CO_2 at 37°C. Transient transfections were performed using the Lipofectin reagent (Invitrogen) according to the manufacturer's protocol or calcium phosphate method. Cells were harvested 24–48 h later for analysis.

Glutathione S-Transferase (GST)-Fusion Protein Pull-Down Assay

GST pull-down analysis was performed essentially as described previously (Lin *et al*., 2002). In brief, 293T cells transfected with ARL4D or mutants were lysed in radioimmunoprecipitation assay (RIPA) buffer containing 50 mM Tris-HCl, pH 7.4, 150 mM NaCl, 1% NP-40, 0.5% sodium deoxycholate, 0.1% SDS, 50 μg/ml *Nα*-*p*-tosyl-L-lysine chlorometyl ketone, 1 mg/ml benzamidine, and 1 μg/ml each pepstatin A, aprotinin, antipain, and leupeptin. The lysates were incubated with 10 μg of GST or GST-ARNO coupled to glutathione beads for 3 h at 4°C. The beads were then washed three times with the RIPA buffer, and the bound protein was analyzed by Western blot.

Coimmunoprecipitation

293T or COS-7 cells were cotransfected with ARL4D and FLAG-ARNO constructs by the calcium-phosphate method. After 48 h, cells were treated with 2 mM dithiobis succinimidylpropionate (DSP; Pierce Chemical, Rockford, IL), a thiol-cleavable cross-linker, to stabilize the protein complex, and lysed in NP-40 lysis buffer (50 mM Tris-HCl, pH 7.4, 150 mM NaCl, and 1% NP-40). Lysates were cleared by centrifugation at 13,000 × *g* for 10 min at 4°C, incubated with M2 anti-FLAG affinity gel (Sigma-Aldrich) for 2 h at 4°C, and then washed three times in NP-40 lysis buffer and once in RIPA buffer. The coimmunoprecipitated proteins were analyzed by Western blot.

Immunofluorescence Microscopy

Cells were fixed in 4% paraformaldehyde in phosphate-buffered saline (PBS) for 15 min and permeabilized with 0.01% Triton X-100 and 0.05% SDS in PBS for 5 min, and blocked with blocking buffer (0.1% saponin, 0.2% bovine serum albumin [BSA] in PBS) for an additional 30 min. Cells were incubated with primary antibodies in blocking solution for 1 h. After extensive washing with PBS, cells were incubated with the Alexa Fluor-conjugated secondary antibodies in blocking solution for 1 h and mounted in 90% glycerol in PBS containing 1 mg/ml *p*-phenylenediamine. For competition experiments, diluted primary antibody was preincubated overnight with equal amounts of immunogen (immunized peptide dissolved in DMSO) or a control peptide.

The plasma membrane localization of ARNO was determined as described previously (Ueda *et al*., 2007). The ARNO membrane localization was evaluated by the fluorescence intensity profile of a typical line scan. The ratios of the average of two fluorescence signals of the plasma membrane to the average signal of the cytosol were measured using Axiovision 4.6 software (Carl Zeiss, Thornwood, NY). In the present study, we defined plasma membrane translocation as a ratio of >1.0. At least 50 different cells were analyzed for each condition. Results are the means ± SD of three independent experiments.

The quantification of F-actin fluorescence was performed as described previously (Poupel *et al*., 2000; Yamashiro *et al*., 2001). F-actin was stained with Alexa Fluor 594-conjugated phalloidin (Invitrogen). Mock-transfected, ARL4D, ARNO, or ARF6 mutant-expression cells were double labeled with the antibody and fluorescent phalloidin. Phalloidin-stained images were taken under the same conditions, and any images showing intensity saturation were excluded from analysis. The area around each cell was delineated, and the mean fluorescence intensity was measured in pixels. Background fluorescence was obtained from a cell-free field of each image and subtracted. Cells expressing exogenous proteins were randomly selected, and mean fluorescent intensities (to compensate for differences in cell size) of phalloidin staining were quantified using the Axiovision 4.6 software (Carl Zeiss). More than 50 cells were examined in each group, and two independent experiments were performed. The results were presented as the mean of the fluorescence intensity for each group of cells ± SD.

For stimulation with EGF, cells were serum starved for 14 h, and 100 ng/ml EGF (Upstate Biotechnology, Lake Placid, NY) was added for 10 min at 37°C. To inhibit PI3K-Akt activation, serum-starved cells were pretreated with 100 nM wortmannin or 1 μM LY294002 (Calbiochem, San Diego, CA) for 1 h, and then they were incubated with EGF in the continuous presence of wortmannin and LY294002. The phosphorylation level of Akt (Ser473) was used to confirm the inhibition of PI3K-Akt activation in each experiment. The staining was examined with a Zeiss Axioplan 2 fluorescence microscope (Carl Zeiss) with a 40×/1.3 numerical aperture (NA) oil objective lens. The images were acquired with a charge-coupled device (CCD) camera (AxioCam HRm; Carl Zeiss) operated by the Axiovision imaging software (Carl Zeiss). Some slides were optically sectioned, and the out-of-focus signals were removed using the ApoTome system (Carl Zeiss). The Apotome system provides an optical section slice view reconstructed from fluorescent samples, by using a series of "grid projection" acquisitions to reject signals belonging to regions of the sample that were outside the best focus position of the microscope. For confocal microscopy, cells were viewed on a Nikon C1 confocal microscope or LSM 510 META laser confocal microscope (Carl Zeiss) with 60×/1.4 NA oil objective lens and 488- or 543-nm lasers. Pinholes were set to scan layers <1 μm, at a resolution of 1024 × 1024 pixels. Both projection view and optical sections were processed digitally using CLSM5 Zeiss Browse Image software. Figures were assembled and labeled using Adobe Photoshop 7.0 (Adobe Systems, Mountain View, CA).

Small Interference RNA (siRNA)

Twenty one-nucleotide (nt) RNA duplexes were purchased from Dharmacon RNA Technologies (Lafayette, CO) for targeting ARL4D or from Ambion (Austin, TX) for targeting ARNO. The sequences of designed siRNAs are as follows (only sense sequences are shown): ARL4D siRNA, 5′-GGGAACCACUUGACUGAGAUU-3′; and ARNO siRNA, 5′-GAUGGCAAUGGGCAGGAAGtt-3′. Control siRNA (nontargeting siRNA pool) were purchased from Dharmacon RNA Technologies. Sixty percent confluent COS-7 or HeLa cells were transfected with siRNA at 100 nM concentration by using Lipofectamine 2000 reagent (Invitrogen) according to the manufacturer's protocol. Cells were harvested after 48 h for immunoblotting and immunofluorescence assays.

Subcellular Fractionation

Subcellular fractionation was performed according to a method described previously (Fournier *et al*., 2005), with a slight modification. HeLa cells were washed with PBS, resuspended in homogenization buffer (0.25 M sucrose, 1 mM EDTA, and 20 mM HEPES-KOH, pH 7.4) and incubated on ice for 15 min before disruption of cells by passing through 26-gauge needle 35 times until ~70% of the cells were broken. All processing steps were performed at 4°C. After low-speed centrifugation (800 × *g*; 6 min) to isolate nuclei and unbroken cells, the postnuclear supernatant (PNS) was then centrifuged at 100,000 × *g* for 1 h to separate into crude cytosolic and membrane fractions. The membrane pellet and 10% PNS were resuspended in the cytosol volume of homogenization buffer, precipitated with trichloroacetic acid. The sedimented materials were resuspended in SDS sample buffer to the same volume, and an equal volume of different fraction was subjected to SDS-PAGE and Western blot analysis using various antibodies.

For ARNO translocation assay, transfected COS-7 cells (~1 × 10^6 cells) were harvested, washed with PBS, and treated with 1 mM DSP, and then the cytosol and membrane fractions of COS-7 cells were prepared using a CNM compartment protein extraction kit (BioChain Institute, Hayward, CA) according to the manufacturer's instructions.

Pull-Down Assay for ARF6-GTP

The activation levels of expressed ARF6 were assayed as described previously (Santy and Casanova, 2001). COS-7 cells grown in 10-cm dishes were cotransfected with the indicated constructs and lysed in 1 ml of ice-cold lysis buffer (50 mM Tris-HCl, pH 7.5; 100 mM NaCl; 2 mM $MgCl_2$; 0.1% SDS; 0.5% sodium deoxycholate; 1% Triton X-100; 10% glycerol, 50 μg/ml *Nα*-*p*-tosyl-L-lysine chlorometyl ketone, 1 mg/ml benzamidine; and 1 μg/ml each pepstatin A, aprotinin, antipain, and leupeptin). Cell extracts were incubated with 20 μg of glutathione Sepharose-bound GST-GGA3 (a.a. 1-316) for 1 h at 4°C. The beads were then washed three times with 50 mM Tris-HCl, pH 7.5, 100 mM NaCl, 2 mM $MgCl_2$, 1% NP-40, and 10% glycerol. Bound proteins were analyzed by immunoblotting using ARF6 or myc antibodies. Immunoblots were scanned, and the GTP-bound ARF6 precipitated with GST-GGA3 was normalized to total ARF levels in the lysates to compare ARF6-GTP levels in cells transfected with the indicated constructs.

Migration Assays

Haptotactic migration assay were performed using a modified Boyden chamber assay, essentially as described previously (Palacios *et al*., 2001). The lower surface of Transwell polycarbonate membranes (6.5 mm diameter, 8-μm pore size; Corning Life Sciences, Acton, MA) were coated with fibronectin (10 μg/ml in DMEM) overnight at 4°C. The membrane was washed in PBS to remove excess ligand, and the lower chamber was filled with 600 μl of migration medium (DMEM with 1% BSA or 10% FBS). Cells were serum starved for 16 h, and then 10^5 cells were suspended in 0.1 ml of DMEM containing 1% BSA were added to the upper chamber and allowed to migrate to the lower side for 6 h. Nonmigratory cells were removed using a cotton

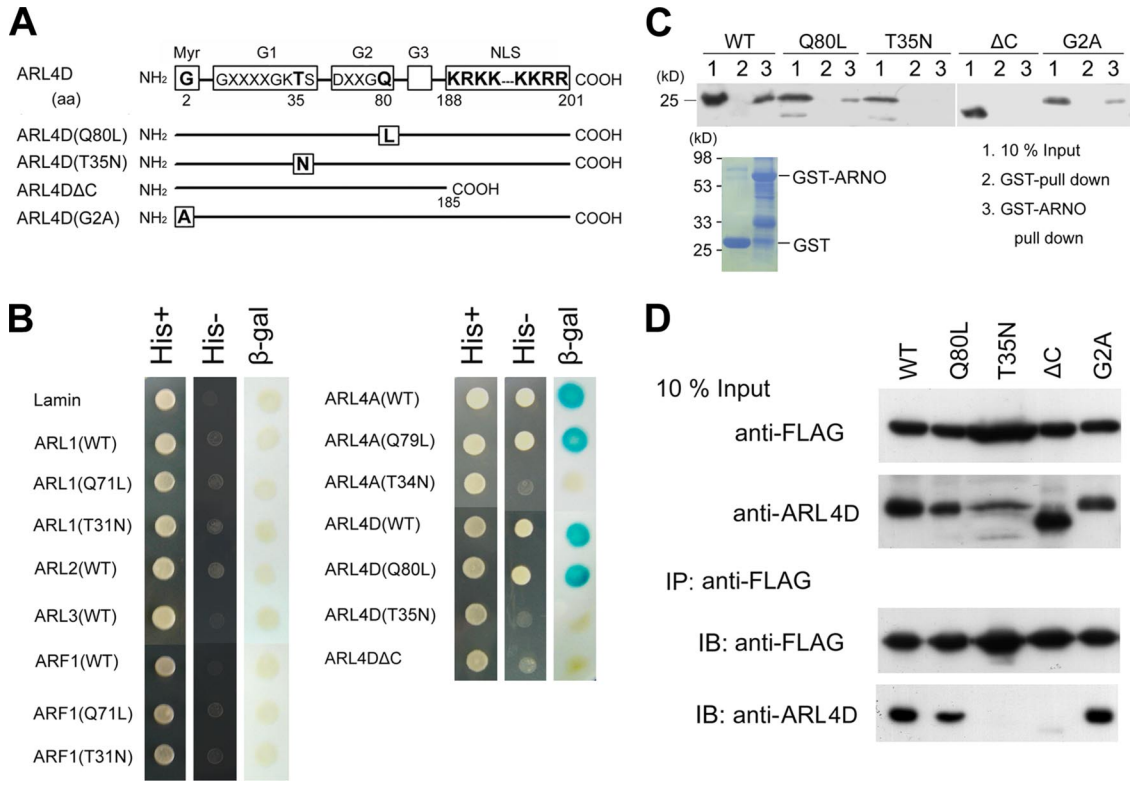

Figure 1. ARNO interacts with ARL4D. (A) Schematic representation of ARL4D molecule and mutants. G1–G3 are conserved regions important for binding to phosphate/Mg^{2+} and the guanine base. ARL4D(Q80L) is a putative GTPase-defective mutant, and it is predicted to exist in the GTP-bound active form. ARL4D(T35N) is a putative GTP-binding-defective mutant, and it is predicted to be in a GDP-bound form. ARL4DΔC lacks 16 a.a. (a.a. 186-201) at the C terminus, which contain the bipartite NLS. ARL4D(G2A) is a *N*-myristoylation–deficient mutant. (B) ARL4D and ARL4A interacted with ARNO in a yeast two-hybrid system. Yeast reporter strain L40 cotransformed with the Gal4 AD fusion constructs of ARNO and the LexA BD fusion of the indicated constructs were grown on synthetic histidine-containing medium lacking leucine and tryptophan (His+ plate) and assayed for β-galactosidase activity by a filter assay. Colonies from His+ plates were also grown on His-minus selective medium lacking histidine, leucine, and tryptophan (His− plate) for a growth assay. (C) ARL4D coprecipitated with ARNO in vitro. Lysates of 293T cells expressing ARL4D or its mutants were incubated with either GST or GST-ARNO immobilized on glutathione beads. Bead-bound ARL4D was probed using anti-ARL4D antibody. Ten percent of the cell lysate (Input) is shown for each of the experiments. The equal input of GST fusion proteins used in the assay and visualized by Coomassie staining is shown on the bottom. (D) Interaction between ARL4D and ARNO. 293T cells cotransfected with ARL4D constructs and FLAG-ARNO were lysed and immunoprecipitated with anti-FLAG M2 affinity agarose gel. Bound proteins were separated by SDS-PAGE and subjected to immunoblot with anti-FLAG and anti-ARL4D antibodies. Ten percent of the cell lysate (Input) was loaded to show the expression level.

swab, whereas migratory cells were fixed with 4% formaldehyde, stained with 1% crystal violet and count by phase-contrast microscopy by using a microscope (Eclipse TS-100; Nikon, Tokyo, Japan) equipped with a digital camera (DS-5M; Nikon). Migratory cells in five fields per well (Nikon Plan Fluor 10 × 0.30 objective) were counted for two individual wells per condition.

For wound-healing migration assays, cells were seeded on six-well plates at a density of 7×10^5 cells/well in culture medium. Thirty hours after seeding, confluent cells were scratched with a fine pipette tip, washed with PBS, and time-lapse microscopy was performed using a microscope (Axiovert 200M; Carl Zeiss) equipped with a temperature and CO_2 controller. Cell movement was recorded at 20-min intervals over 18 h with a CCD video camera (CoolSNAP HO; Roper Scientific, Trenton, NJ) operated by MetaMorph 7.0 image analysis software (Molecular Devices, Sunnyvale, CA). Quantitation of cellular migration was performed as described previously (Santy and Casanova, 2001). The area covered by the monolayer (decreased wound area) was traced and measured using MetaMorph 7.0 software.

RESULTS

Identification of Cytohesin-2/ARNO as an ARL4D Interactor

To identify potential effectors of ARL4D, we used a yeast two-hybrid system and used the ARL4D(Q80L), a putative GTP-bound form of ARL4D, as bait to screen a mouse embryonic cDNA library. We identified several candidate genes, including eight independent clones for cytohesin-2/ARNO. We next assessed specificity among ARF/ARL family members by yeast two-hybrid assays (Figure 1, A and B). Our data showed that ARNO interacted specifically with ARL4D and ARL4A, but not with ARF1 or other ARLs. Furthermore, ARNO interacted with ARL4D(WT), ARL4A(WT), ARL4D(Q80L), and ARL4A(Q79L), but not with ARL4DΔC, the GTP-binding-defective mutant ARL4D(T35N) or ARL4A(T34N). These results indicated that the interactions were specific, nucleotide dependent, and involved the C terminus of ARL4D.

To confirm the ARL4D and ARNO interaction, we performed in vitro GST pull-down assays. We tested whether purified, bacterially expressed GST-ARNO could bind to ARL4D or its mutants (Figure 1C). GST-ARNO pulled down ARL4D, ARL4D(Q80L), and ARL4D(G2A), but not ARL4D(T35N) or ARL4DΔC. GST alone failed to pull down ARL4D constructs. Next, we used coimmunoprecipitation experiments to demonstrate that ARL4D interacts with ARNO. Proteins immunoprecipitated from lysates of 293T cells coexpressing ARL4D or mutants and FLAG-ARNO with anti-FLAG M2 affinity gel were immunoblotted with antibodies against ARL4D or FLAG. As shown in Fig-

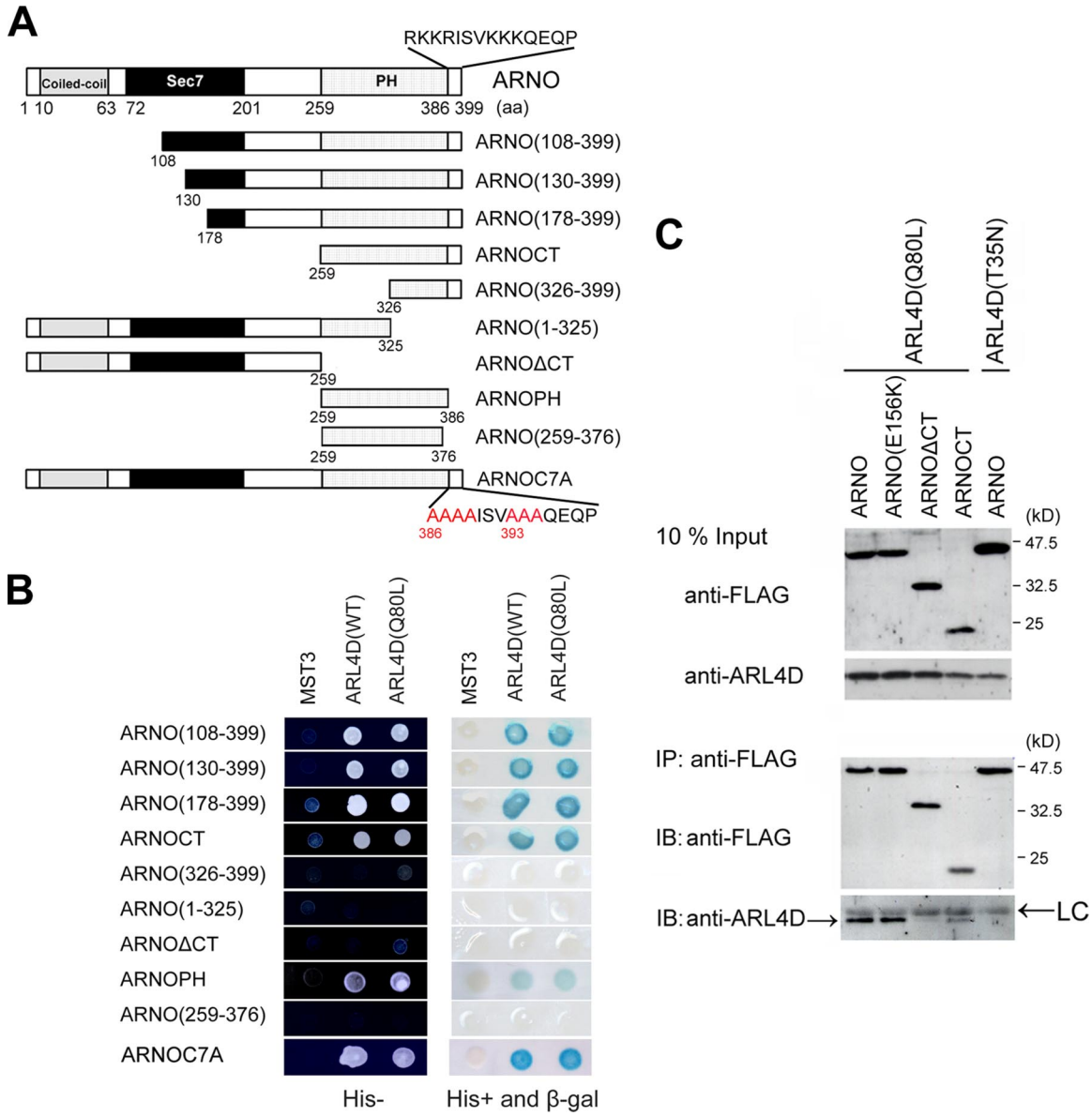

Figure 2. The PH domain of ARNO interacts with ARL4D. (A) Schematic representation of ARNO and its deletion mutants. ARNO contains a coiled-coil domain (a.a. 10-63), Sec7 domain (a.a. 72-201), PH domain, and polybasic c domain (a.a.386-399). (B) ARL4D and its activated mutants fused to the DNA BD of LexA were cotransformed with deletion mutants of ARNO fused to the Gal4 AD into yeast strain L40, and the transformants were tested for their ability to grow in the absence of histidine (left) and to express β-galactosidase (right). Mammalian STE20-like protein kinase 3 (MST3) was a negative control. (C) Interaction of ARL4D and ARNO is mediated by the C terminus of ARNO. COS-7 cells transfected with the indicated expression vectors were treated with the reducible cross-linker DSP before cells were lysed. Proteins immunoprecipitated from cell lysates with an anti-FLAG M2 affinity agarose gel were separated by SDS-PAGE and immunoblotted with anti-ARL4D or anti-FLAG antibodies. ARL4D(Q80L) was selectively coimmunoprecipitated with FLAG-ARNO constructs containing the C-terminal PH domain and polybasic c domain. The arrows indicate the immunoglobulin light chain (LC) of antibody.

ure 1D, ARL4DWT, ARL4D(Q80L), or ARL4D(G2A), but not ARL4D(T35N) or ARL4DΔC, was coimmunoprecipitated with FLAG-ARNO. Thus, we demonstrated interactions of recombinant ARNO and ARL4D that were nucleotide dependent and involved in the C-terminal NLS domain by using proteins synthesized in bacteria or in 293T cells.

The PH Domain and the Polybasic C Domain of ARNO Are Both Necessary and Sufficient for Interaction with ARL4D

All ARNO clones isolated from the yeast two-hybrid screening contained an intact PH domain and partial Sec7 domain, suggesting that the C-terminal PH domain of ARNO may be involved in the interaction with ARL4D. To identify the specific domains of ARNO responsible for this interaction, a series of ARNO-deletion mutants was generated (Figure 2A) and tested for the ability to interact with ARL4D in yeast two-hybrid assays (Figure 2B). We found that the C-terminal 140 amino acids (ARNOCT) alone were sufficient for the interaction; the N-terminal coiled-coil and central Sec7 domains were not required. ARL4D interaction with the ARNO PH domain (ARNOPH) was much weaker than that of the C-terminal PH domain and polybasic c domain

(ARNOCT) (Figure 2B), indicating that, besides the PH domain, the C-terminal polybasic c domain is also important. The C-terminal polybasic stretch of cytohesin-1 and ARNO was reported to be important for its collaboration with the PH domain in membrane recruitment and phospholipids PIP_3 binding (Nagel *et al*., 1998a; Macia *et al*., 2000; Dierks *et al*., 2001). To determine whether the basic charge amino acids in the C-terminal polybasic stretch is important for the interaction between ARL4D and ARNO, we used site-directed mutagenesis to generate an ARNO mutant, ARNOC7A, in which the seven basic residues were replaced with alanine. Interestingly, ARNOC7A, like ARNO, showed similar interaction ability for ARL4D (Figure 2B). This result indicates that the C-terminal basic amino acids are not involved in the interaction between ARL4D and ARNO. These constructs were expressed in relatively equal amounts in the transformed yeast (unpublished data).

By coimmunoprecipitation, we further showed that ARL4D(Q80L) was coimmunoprecipitated with FLAG-ARNO and FLAG-ARNOCT, but not FLAG-ARNOΔCT (Figure 2C). Thus, our results demonstrate that the PH domain and polybasic c domain of ARNO are necessary and sufficient for interaction with ARL4D.

ARNO Does Not Catalyze Nucleotide Exchange on ARL4D

ARNO has previously been shown to catalyze guanine nucleotide exchange on ARF6 in vitro (Frank *et al*., 1998a). To determine whether ARL4D is a substrate of ARNO, we measured the ability of ARNO to catalyze the binding of GTPγS on ARF6 and ARL4D. Consistent with the previous observation (Frank *et al*., 1998a), ARF6 undergoes spontaneous nucleotide exchange even in the absence of ARNO and addition of ARNO results in a stimulation of GTPγS binding (Supplemental Figure S1A and S1B). However, no stimulation of GTPγS binding was observed when using ARL4D as substrate. Our data indicated that ARNO could not catalyze nucleotide exchange on ARL4D in the GTPγS binding assay.

Localization of ARL4D at the Plasma Membrane Is GTP Dependent

Our previous studies showed that N-terminally enhanced green fluorescent protein (EGFP)-tagged ARL4D is located in nuclei and partially in nucleoli and can interact with importin-α through its C-terminal bipartite NLS (Lin *et al*., 2002). However, ARL4D has a myristoylation site at its N terminus and a NLS in its C terminus; thus, epitope tags at either end might sterically hinder and change its conformation, localization, and function. To examine the physiological phenotype of ARL4D, we first used two unique peptides (peptide N corresponding to a.a. 2-18 and peptide B a.a. 139-155 of ARL4D) to generate peptide-specific antibodies (Supplemental Figure S2A). A Blast search using the peptide sequences of ARL4D-N and ARL4D-B did not reveal any homologous peptides. The antibody against peptide B was more sensitive in detecting purified recombinant human ARL4D in low nanogram amounts, whereas no reaction was detected with 100 ng of recombinant human ARL4A, ARF1, or ARF6 proteins (Supplemental Figure S2B). Using this antibody, endogenous ARL4D was detected in three cell lines (Supplemental Figure S2C). The detected ~25-kDa band was similar in size to recombinant ARL4D protein expressed in HeLa cells.

To determine the subcellular localization of ARL4D, we first analyzed overexpression of ARL4D and its mutants in transiently transfected COS-7 cells by indirect immunofluorescence microscopy (Figure 3A). The stacked images were obtained by using a confocal microscope. The single plane images of transfected cells are shown in Supplemental Figure S3. Interestingly, ARL4D was detected at the plasma membrane, in addition to the nucleus and cytoplasm. Like ARL4D(WT), ARL4D(Q80L) was detected in the nucleus and diffusely throughout the cytoplasm but concentrated most intensely at the plasma membrane, where it associated with areas of membrane folding or ruffles along the periphery of the cell. Notably, cells transfected with ARL4D(Q80L) also demonstrated membranous protrusion structures from their dorsal surface, and ARL4D(Q80L) was also concentrated within these structures. Nuclear, perinuclear punctate, and diffuse cytoplasmic labeling, but much less plasma membrane-associated signals, were detected in cells expressing ARL4D(T35N). Our results indicated that subcellular localization of ARL4D was guanine nucleotide dependent. We further showed that ARL4D(G2A), containing Ala substituted for Gly at position 2, was diffusely distributed in the cytoplasm (Figure 3A), indicating that N-terminal myristoylation is important for association with the plasma membrane.

We next used the ARL4D antibody to detect endogenous ARL4D. Figure 3B shows the result of an immunoblot antibody competition analysis of total HeLa cell lysate. The detection of a 25-kDa protein was abolished by preincubation of the antibody with the ARL4D-B peptide immunogen but not with ARL4D-N peptide. Moreover, endogenous ARL4D distributed mainly in the membrane fraction after cytosol-membrane fractionation of HeLa cells (Figure 3C). We also observed that an ~42-kDa band on immunoblots, which was only seen with nuclear fractions, was abolished by the addition of a specific ARL4D-B antigen (Figure 3, B and C). Whether the ~42-kDa band is the source of the nuclear staining due to endogenous proteins needs to be further investigated. We also examined the subcellular localization of endogenous ARL4D in interphase HeLa cells. Endogenous ARL4D, like overexpression of ARL4D, was detected at the plasma membrane, in addition to the nucleus and cytoplasm (Figure 3D). PMCA was used as a control. The signals of ARL4D were abolished when the antibody was preincubated with the ARL4D-B peptide used for immunization, but not with DMSO or ARL4D-N peptide.

Both the PH Domain and Polybasic c Domain, but Not GEF Activity of ARNO, Are Required for ARL4D-Induced Recruitment of ARNO to the Plasma Membrane

The PH domain of ARNO is required for its membrane targeting or translocation (Venkateswarlu *et al*., 1998). We examined whether ARL4D could affect the subcellular localization of ARNO in transiently transfected COS-7 cells. Figure 4A showed that FLAG-ARNO was detected as a diffuse signal throughout the cytoplasm and was not clearly observed at the periphery plasma membrane in COS-7 cells. Coexpression of FLAG-ARNO and ARL4D(WT) or its mutants reveals that part of FLAG-ARNO was colocalized with ARL4D(WT) or ARL4D(Q80L) at plasma membrane ruffles and dorsal membranous protrusions. This translocation of ARNO was not observed in cells coexpressing ARL4D(G2A) or ARL4D(T35N) (Figure 4B). We confirmed the effect of ARL4D(Q80L) on ARNO translocation to the membrane fraction by subcellular fractionation (Supplemental Figure S4). We also observed similar effects of ARL4D on ARNO in HeLa and Madin Darby canine kidney (MDCK) cells (unpublished data). The localization of ARL4D or its mutants was not altered when coexpressed with FLAG-ARNO (compare with Figures 3 and 4B). Quantitation of the ARNO fluorescence signal confirmed that ARL4D(WT) or ARL4D(Q80L) induced ARNO redistribution to the plasma membrane (Figure 4, C and D). Moreover, overexpression of ARF1(Q71L) or ARL1(Q71L) did

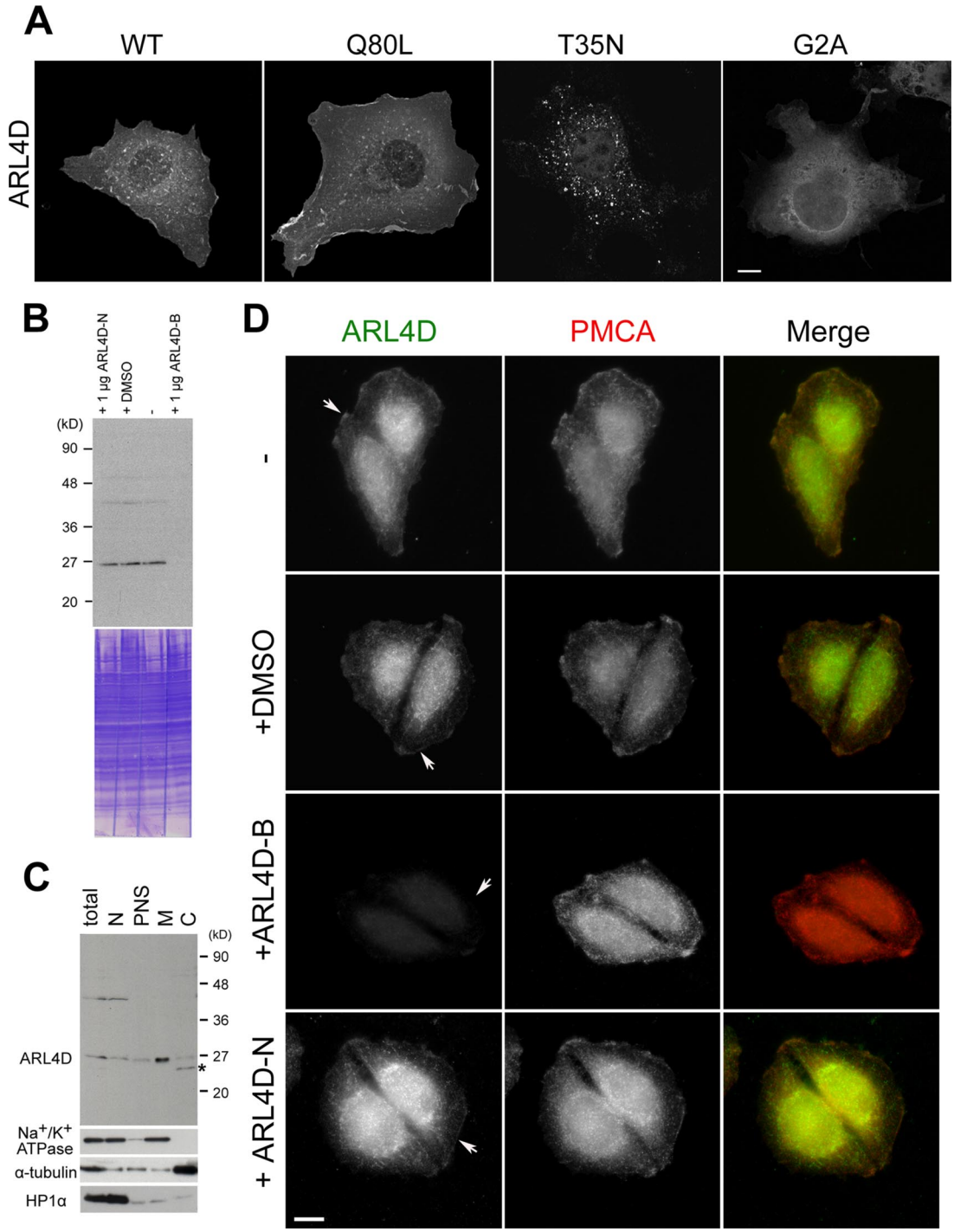

Figure 3. Subcellular localization of ARL4D and its mutants. (A) Localization of overexpressed untagged ARL4D. COS-7 cells grown on coverslips were transiently transfected with plasmids encoding ARL4D or its mutants. Forty-eight hours after transfection, cells were fixed, permeabilized, and processed for immunofluorescence with anti-ARL4D antibody. The stacked images were obtained by using a confocal microscope. (B) Detection of endogenous ARL4D by immunoblotting. Total HeLa cell lysate was separated by SDS-PAGE and probed with anti-ARL4D-B antibody alone, or anti-ARL4D-B competed by 1 μg of immunized ARL4D-B peptide, or nonimmunized ARL4D-N peptide dissolved in DMSO. DMSO was used as a mock control. (C) Subcellular distribution of endogenous ARL4D by fractionation. HeLa cells were homogenized and nuclear (N), PNS, cytosolic (C), and membrane (M) fractions prepared as described in *Materials and Methods*. Equivalent amounts of proteins were separated by SDS-PAGE and analyzed by Western blot by using specific antibodies against ARL4D-B, HP1α (nuclear marker), α-tubulin (cytosol marker), and Na^+/K^+ATPase (membrane marker). Asterisk (*) indicates a nonspecific band detected in cytosolic fraction. This band might be a degradation product from an unknown protein (~40-kDa), which was cross-reacted with the ARL4D antibody in the total cell lysate. (D) Subcellular localization of endogenous ARL4D in HeLa cells. Endogenous ARL4D or plasma membrane calcium pump pan PMCA ATPase was detected by immunofluorescence staining with anti-ARL4D-B or anti-PMCA antibody, respectively. The plasma membrane labeling (arrow) was abolished when the antibody was preincubated with ARL4D-B peptide but not by DMSO (mock control) or ARL4D-N peptide. Bar, 10 μm. Peptide competition assays were performed as described in *Materials and Methods*.

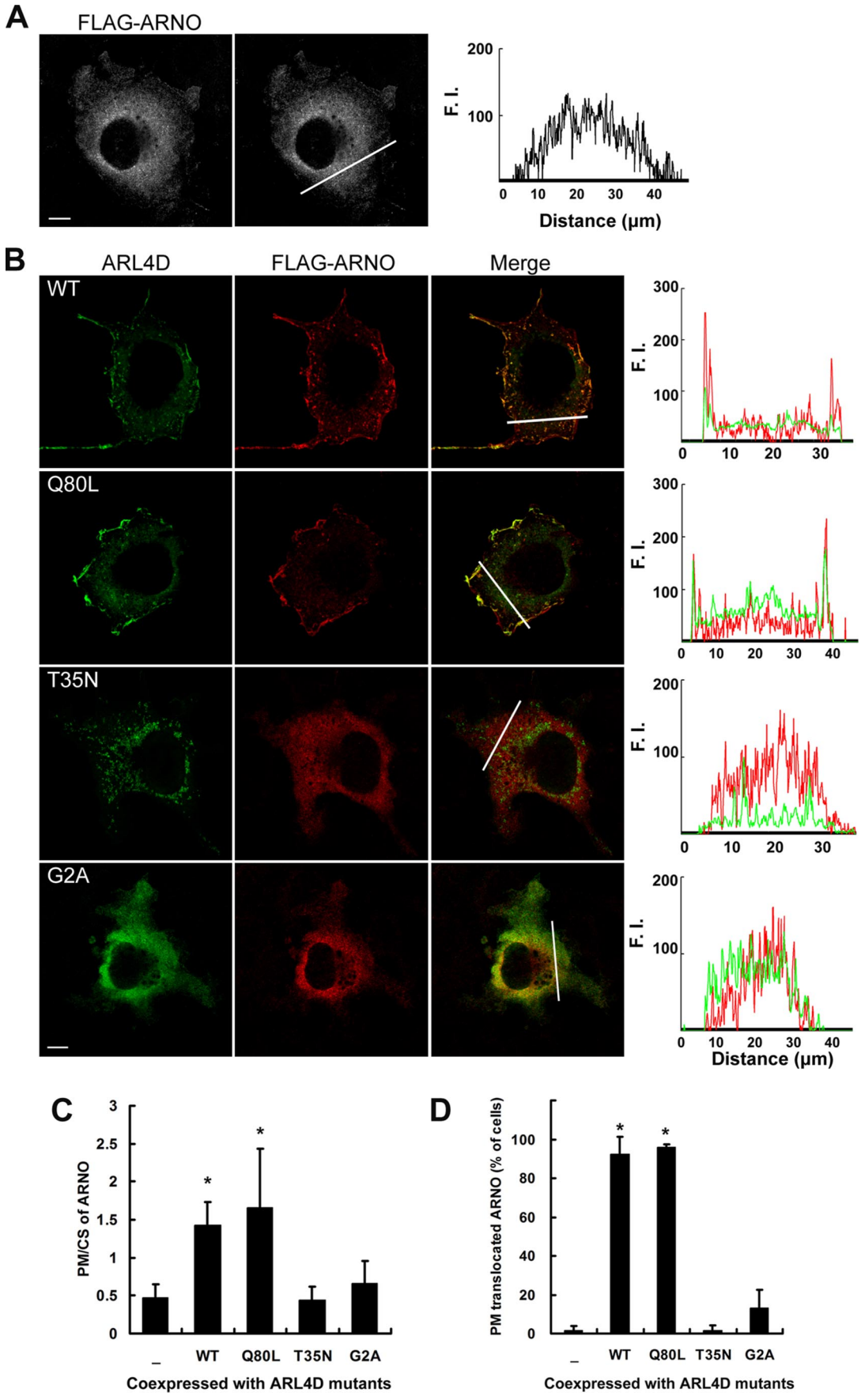
A
FLAG-ARNO
F. I.
200
100
0 10 20 30 40
Distance (μm)
B
ARL4D
FLAG-ARNO
Merge
WT
Q80L
T35N
G2A
F. I.
300
200
100
0 10 20 30
0 10 20 30 40
Distance (μm)
C
PM/CS of ARNO
3
2.5
2
1.5
1
0.5
0
*
*
_ WT Q80L T35N G2A
Coexpressed with ARL4D mutants
D
PM translocated ARNO (% of cells)
100
80
60
40
20
0
*
*
_ WT Q80L T35N G2A
Coexpressed with ARL4D mutants

Figure 4.

not affect the distribution of FLAG-ARNO (unpublished data). Collectively, these data indicate that ARL4D can induce ARNO redistribution to the plasma membrane and this effect is GTP dependent.

We next examined whether the PH domain or polybasic c domain is required for inducing redistribution of ARNO by ARL4D. COS-7 cells were transfected with ARNOΔCT or ARNOCT and/or ARL4D(Q80L). Similar to that of wild-type ARNO, the localization of ARNOΔCT or ARNOCT is detected in the cytoplasm, and it did not seem to concentrate at the lateral margins (Supplemental Figure S5A and S5B). Although ARL4D(Q80L) could not induce redistribution of ARNOΔCT to the plasma membrane, ARNOCT and ARNOC7A were translocated to ARL4D(Q80L)-enriched plasma membrane in a manner similar to full-length FLAG-ARNO (Supplemental Figure S5B and S5C). Moreover, ARL4D(Q80L) can only recruit less amounts of ARNOPH than full-length ARNO to the plasma membrane (Supplemental Figure S5D). Our data demonstrate that ARL4D mediates redistribution of ARNO through its C-terminal PH domain and polybasic c domain.

ARNO is a GEF for ARF1 and ARF6 (Chardin *et al*., 1996; Frank *et al*., 1998a); thus, we were interested to learn whether ARL4D-regulated translocalization of ARNO is dependent on ARNO GEF activity. To test this, we constructed a catalytically inactive GEF form of ARNO, ARNO(E156K). When expressed in COS-7 cells, ARNO(E156K) exhibited a distribution similar to that of wild-type ARNO (Supplemental Figure S6A). ARNO(E156K) was coprecipitated by ARL4D(Q80L) (Figure 2C), and, like the wild-type ARNO, ARNO(E156K) was also recruited to the ARL4D(Q80L)-enriched plasma membrane region (Supplemental Figure S6B). Moreover, coexpression of ARNO(E156K) or down-regulation of endogenous ARNO by siRNA in COS-7 cells did not affect the distribution of ARL4D(WT) (unpublished data). These data suggest that induced redistribution of ARNO by ARL4D does not require ARNO GEF activity.

ARL4D Promotes Activation of ARF6

Translocation of ARNO to the plasma membrane is a critical event for ARNO GEF activity and ARF6 activation. We examined whether ARL4D-induced ARNO membrane-targeting can promote the activation of ARF6. We showed in Figure 5A that cells cotransfected with ARF6 and ARL4D(Q80L) exhibited colocalization along plasma membrane ruffles and protrusions. Conversely, ARF6 showed little or no colocalization with ARL4D(T35N). We carried out a pull-down assay to detect ARF6 states by using a GST fusion construct containing the VPS27, Hrs, and STAM- and ARF-binding domains of GGA3 (Santy and Casanova, 2001). ARF6(Q67L) bound to GST-GGA3 was used as a control (Figure 5B). In COS-7 cells, wild-type ARF6-myc was coexpressed with either hemagglutinin (HA)-ARNO, ARL4D(Q80L), or ARL4D(T35N). ARL4D(Q80L), but not ARL4D(T35N), stimulated ARF6 activation. Consistent with a previous report (Santy and Casanova, 2001), ARF6 activation was stimulated by ARNO (Figure 5B). Moreover, cells coexpressed with HA-ARNO and ARL4D(Q80L) increased the GTP-bound form of endogenous ARF6 (Figure 5C). Together, these results indicate that ARL4D recruits ARNO to the plasma membrane and thus promotes activation of ARF6.

ARL4D(Q80L) Induces Disassembly of Actin Stress Fibers

Both ARNO and ARF6 have been demonstrated to modulate the assembly and organization of the actin cytoskeleton (Radhakrishna *et al*., 1996; D'Souza-Schorey *et al*., 1997; Frank *et al*., 1998b; Boshans *et al*., 2000). Next, we investigated whether the downstream effect of ARL4D-induced ARNO translocation and ARF6 activation might be involved in the organization of the actin cytoskeleton (Figure 6). Consistent with previous reports (D'Souza-Schorey *et al*., 1997; Frank *et al*., 1998b; Boshans *et al*., 2000), expression of ARNO, but not the catalytically inactive ARNO(E156K) mutant, resulted in the reduction of stress fibers, and a decrease in actin stress fibers was elicited by overexpression of ARF6(Q67L), but not ARF6(T27N) (Figure 6, A and C). As expected, examination of actin organization in cells expressing ARL4D(Q80L) revealed a loss of stress fibers, and this phenotype was not observed in mock-transfected cells, indicating that the loss of stress fibers is a consequence of ARL4D(Q80L) expression (Figure 6, A and C). A similar phenotype was seen with the expression of relatively higher levels of wild-type ARL4D (Figure 6C; data not shown). Expression of ARL4D(T35N) or ARL4D(G2A) did not result in the reduction of stress fibers (Figure 6, A and C). Quantitative fluorescence analyses for F-actin intensity are shown in Figure 6C. Together, our data indicate that ARL4D(Q80L), similar to ARNO and ARF6(Q67L), induces disassembly of actin stress fibers.

ARL4D Modulates Actin Remodeling through ARNO and ARF6

Having demonstrated that overproduction of ARL4D manipulates the downstream effect in a manner similar to that of ARNO and ARF6, we next examined whether ARL4D may act coordinately with ARNO and ARF6 to modulate actin organization. Two experiments for abolishing GEF activity and reducing the expression level of ARNO helped dissect this possibility. First, cells transfected with ARNO(E156K) showed no effect on stress fiber organization and inhibited the decrease in ARL4D(Q80L)-induced actin remodeling (Figure 6, B and C). Second, we introduced ARNO or ARL4D siRNAs into COS-7 cells, and we showed that expression of endogenous ARNO and ARL4D were markedly reduced when cells were treated with ARNO-specific and ARL4D-specific siRNAs (Figure 6D). These siRNAs were specific, and they did not interfere with expression of other proteins, such as calnexin, α-tubulin, or ARF6. We further used siRNA knockdown to ask whether reduction of ARNO could block ARL4D(Q80L)-mediated actin remodeling. The localization of ARL4D(WT) or ARL4D(Q80L) in ARNO knockdown cells remained unchanged; however, ARL4D(Q80L)-induced stress fiber reduction was significantly decreased (Figure 6E; data not shown). In contrast, reduction of ARL4D had no affect on ARNO-mediated decrease in actin stress fibers (Figure 6F). It clearly demonstrated that ARNO is the direct downstream effector of ARL4D on the actin remodeling. Consistent with the result from ARNO GEF inactivation, an inactive

Figure 4 (cont). ARL4D induces ARNO redistribution to plasma membrane protrusions and ruffles. COS-7 cells were transfected with FLAG-ARNO alone (A) or cotransfected with FLAG-ARNO and ARL4D mutants (B). Cells were fixed, permeabilized, labeled with anti-FLAG M2 and anti-ARL4D antibody and examined by confocal microscopy. Staining intensities measured according to pixel brightness were evaluated by the fluorescence intensity (F.I.) profile of a typical line scan for ARNO in a representative positively stained cell. (C) Quantification of ARNO localization in ARL4D-coexpressing cells. The ratios of the average of the two fluorescence signals of the plasma membrane (PM) to the average signal of the cytosol (CS) were evaluated. (D) Quantification of translocation of ARNO to plasma membrane protrusions and ruffles in ARL4D-expressing cells. The method for quantifying the ARNO plasma membrane localization is described in *Materials and Methods*. At least 50 cells were analyzed for each condition. Results are the means ± SD of three independent experiments. *$p < 0.001$ compared with ARNO alone. Bars, 10 μm.

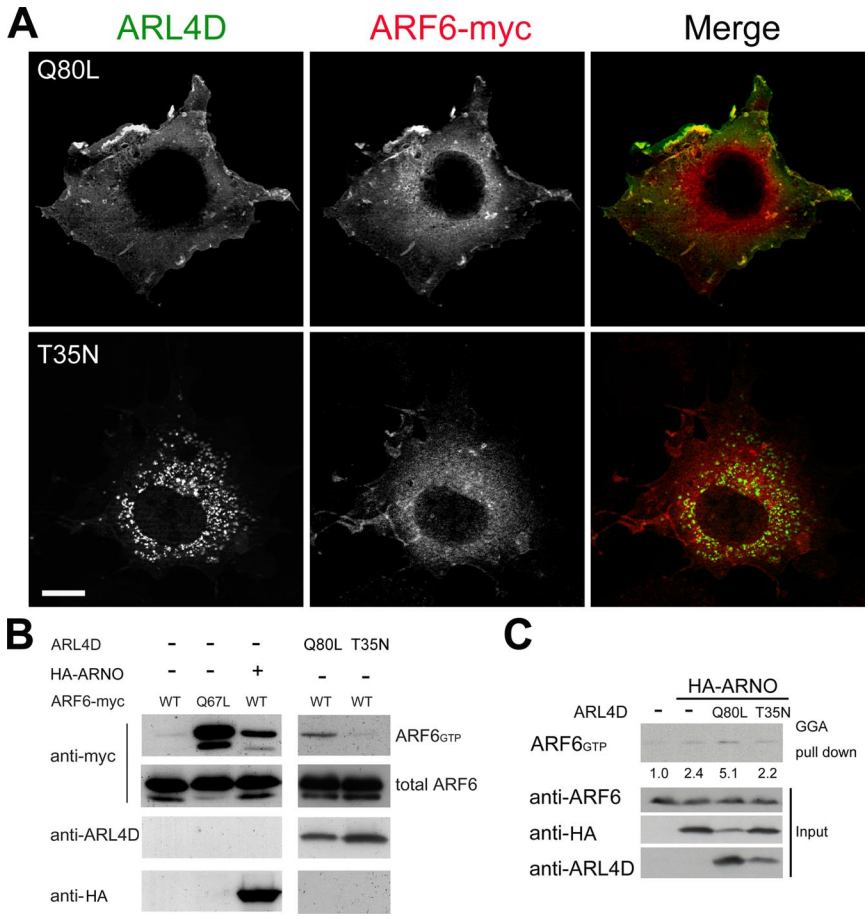

Figure 5. ARL4D promotes activation of ARF6. (A) ARL4D(Q80L) and ARF6 colocalize along plasma membrane ruffles and protrusions. COS-7 cells cotransfected with vectors encoding ARL4D(Q80L) or ARL4D(T35N) together with ARF6-myc were processed for immunofluorescence with ARL4D and myc antibodies and examined by confocal microscopy. Bar, 10 μm. (B) Expression of ARL4D(Q80L) results in increased levels of ARF6-GTP. COS-7 cells transfected with plasmids encoding ARF6-myc and/or the indicated proteins were lysed. ARF6-GTP was precipitated using GST-GGA3 coupled to glutathione beads, and the precipitates were immunoblotted with anti-myc antibody. Samples of cell lysates (2% input) were also immunoblotted with myc, HA, and ARL4D antibodies. (C) Overexpression of HA-ARNO increased endogenous ARF6-GTP in HeLa cells when ARL4D(Q80L) was coexpressed. ARF6-GTP levels were calculated as the ratio of the ARF6-GTP to total ARF6 (5% input), and they are reported relative to that in the absence a HA-ARNO = 1.0.

form of ARF6 (T27N), blocked ARL4D(Q80L)-induced actin remodeling. ARL4D(T35N) did not block ARF6(Q67L)-mediated cytoskeletal rearrangements (Figure 6, B and C) or interfere with the ARNO-mediated reduction of actin stress fibers (Figure 6, B and C). These data demonstrate that ARL4D effects on actin remodeling lie upstream of ARNO and ARF6.

Requirement for ARL4D in Cell Migration

Expression of ARNO or activation of ARF6 stimulates MDCK cell migration (Palacios *et al.*, 2001; Santy and Casanova, 2001), and suppression of ARF6 blocks invasive and migration activities of breast cancer cells (Hashimoto *et al.*, 2004). To investigate the potential role of ARL4D in cell migration, we assessed whether knockdown of the endogenous ARL4D would impair cell motility. We used a Transwell migration assay with control siRNA, ARL4D siRNA, and ARNO siRNA in HeLa cells. The cells were plated in the upper chamber containing filters that had been coated with fibronectin on the underside, and they were allowed to migrate for 6 h. As shown in Figure 7, B and C, HeLa cells transfected with either ARL4D siRNA or ARNO siRNA showed a significantly reduced motility compared with control siRNA. We also used a wound-healing assay to monitor cell migration and obtained similar results. Namely, knockdown of ARL4D or ARNO expression caused a delay in wound closure (Figure 7D). Quantification of the wound area covered by the migrating monolayer cell is shown in Figure 7E. Together, these results provide evidence that ARL4D play a physiological role in cell motility.

ARL4D-induced Translocation of ARNO to the Plasma Membrane Is Independent of PI3-Kinase Signaling

It has been demonstrated that cytohesin-2/ARNO responds to the PI3-kinase signaling cascade through the selectivity of PH domains for binding PIP_3, and cells stimulated with agonists such as epidermal growth factor (EGF), nerve growth factor (NGF), or insulin showed translocation of cytohesin-2/ARNO from the cytosol to the plasma membrane; this redistribution was inhibited by PI3K inhibitors (wortmannin and LY294002) (Venkateswarlu *et al.*, 1998, 2003; Mansour *et al.*, 2002). To investigate whether the effects of ARL4D on inducing redistribution of ARNO to the plasma membrane were dependent on PI3K, we first examined the subcellular localization of ARL4D and ARNO in transfected cells when PI3K activity was stimulated by EGF or was blocked by PI3K inhibitors (Figure 8, A and B). To confirm the inhibition of PI3K–Akt activation, the phosphorylation level of Akt (Ser473) was examined in each experiment (data not shown). As shown in a previous report (Mansour *et al.*, 2002), EGF stimulated plasma membrane ruffling and translocation of ARNO to membrane ruffles (Figure 8A). This translocation of ARNO was abrogated by the addition of wortmannin or LY294002 (Figure 8, A and C). However, the localization of ARL4D at the plasma membrane was not affected by wortmannin or LY294002, indicating that localization of ARL4D is not dependent on PI3K signaling (Figure 8A). Consistent with this finding, ARL4D-mediated redistribution of ARNO to the plasma membrane was not blocked by wortmannin when cells were incubated

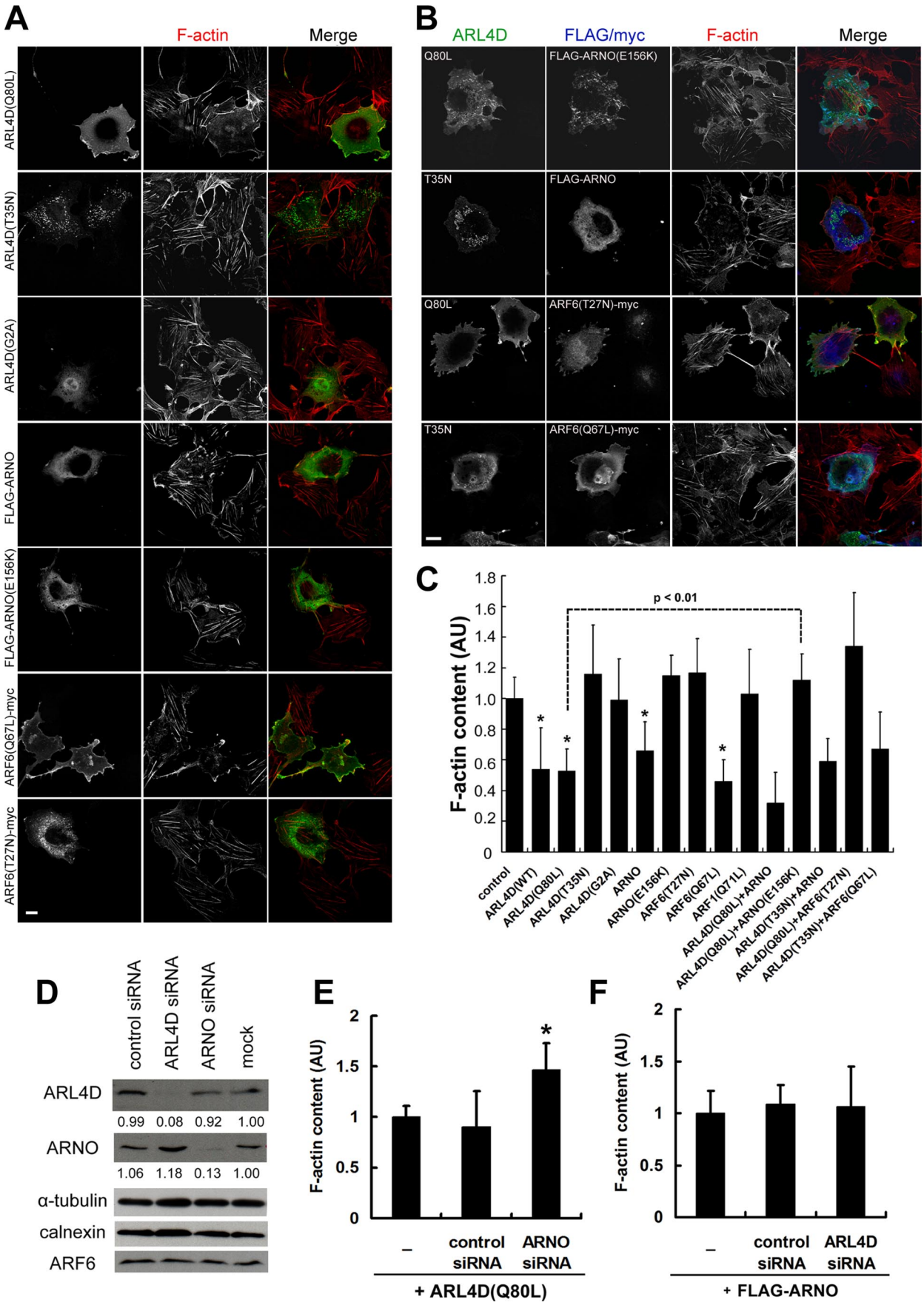
A
F-actin
Merge
ARL4D(Q80L)
ARL4D(T35N)
ARL4D(G2A)
FLAG-ARNO
FLAG-ARNO(E156K)
ARF6(Q67L)-myc
ARF6(T27N)-myc
B
ARL4D
FLAG/myc
F-actin
Merge
Q80L
FLAG-ARNO(E156K)
T35N
FLAG-ARNO
Q80L
ARF6(T27N)-myc
T35N
ARF6(Q67L)-myc
C
F-actin content (AU)
p < 0.01
control
ARL4D(WT)
ARL4D(Q80L)
ARL4D(T35N)
ARL4D(G2A)
ARNO
ARNO(E156K)
ARF6(T27N)
ARF6(Q67L)
ARF1(Q71L)
ARL4D(Q80L)+ARNO
ARL4D(Q80L)+ARNO(E156K)
ARL4D(T35N)+ARNO
ARL4D(Q80L)+ARF6(T27N)
ARL4D(T35N)+ARF6(Q67L)
D
control siRNA
ARL4D siRNA
ARNO siRNA
mock
ARL4D
0.99 0.08 0.92 1.00
ARNO
1.06 1.18 0.13 1.00
α-tubulin
calnexin
ARF6
E
F-actin content (AU)
–
control siRNA
ARNO siRNA
+ ARL4D(Q80L)
F
F-actin content (AU)
–
control siRNA
ARL4D siRNA
+ FLAG-ARNO

Figure 6.

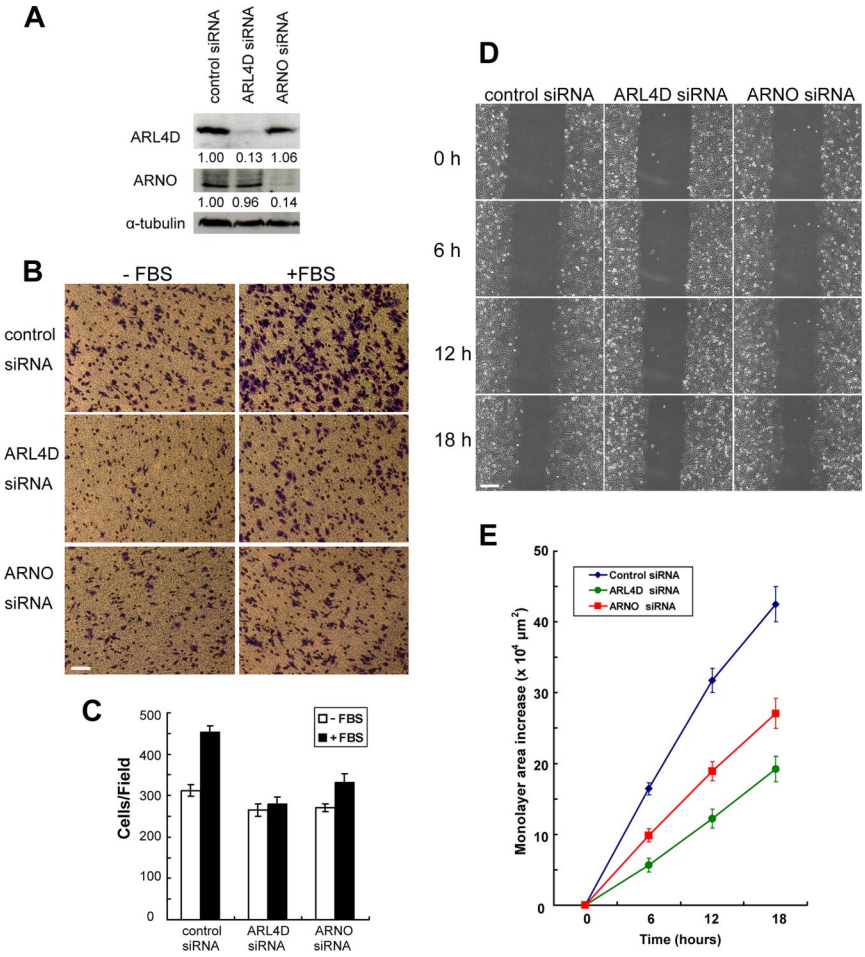

Figure 7. Requirement for ARL4D in cell migration. (A) HeLa cells transfected with ARL4D siRNA, ARNO siRNA, or a control siRNA were lysed 48 h after transfection, and then they were assayed for expression by immunoblotting. (B and C) HeLa cells transfected with the indicated siRNAs were subjected to a Transwell migration assay. Cells were plated in the upper chamber of the filters that had been coated on the underside with fibronectin, and their migrations were assessed in the presence or absence of FBS as indicated. Six hours after plating, cells that had migrated to the underside of the filters were fixed, stained with crystal violet, and counted as described in *Materials and Methods*. Error bars represent the SD of three independent experiments. Bar, 100 μm. (D) Time-lapse microscopy of wound healing migration of HeLa cells transfected with indicated siRNA. Cells were cultured to confluence and then scratched. Cell migration into wounds was monitored and images were captured at the indicated time after wounding. Bar, 200 μm. (E) Quantification of wound-healing migration assays. Migration was measured by calculating the change in the area between migrating cell sheets using MetaMorph software and five repeats per data point. The increase in cellular monolayer area over time is shown. Results are the means ± SD.

Figure 6 (facing page). ARL4D(Q80L) induces actin stress fiber disassembly. (A) COS-7 cells were transfected with an expression vector encoding FLAG-ARNO, FLAG-ARNO(E156K), ARL4D(Q80L), ARL4D(T35N), ARL4D(G2A), ARF6(Q67L)-myc, and ARF6(T27N)-myc, respectively. Forth-eight hours after transfection, cells were fixed and stained with phalloidin to visualize F-actin and with anti-FLAG, ARL4D, or myc antibody. (B) ARNO(E156K) suppressed decrease of stress fibers induced by ARL4D(Q80L) expression. COS-7 cells cotransfected with a combination of either ARL4D(Q80L) and FLAG-ARNO(E156K), ARL4D(T35N) and FLAG-ARNO, ARL4D(Q80L) and ARF6(T27N)-myc, or ARL4D(T35N) and ARF6(Q67L)-myc. Cells were fixed and labeled with anti-ARL4D and FLAG M2 or myc 9E10 antibody and with phalloidin to visualize F-actin. (C) Quantification of the average fluorescence intensity of F-actin in cells expressing the indicated proteins is described in *Materials and Methods*. Data are given as the mean ± SD and expressed as arbitrary units (AU). For each population, at least 50 cells were scored. *$p < 0.05$, calculated by *t* test and compared with control cells. (D) Depletion of ARNO or ARL4D in COS-7 cells by siRNA. Extracts were prepared 48 h posttransfection, and immunoblots were performed with antibodies against ARNO, ARL4D, ARF6, α-tubulin, or calnexin. Relative ARL4D or ARNO expression was compared after setting the ratio of ARL4D or ARNO signal to α-tubulin signal in the mock-transfected cells as 1.0. (E and F) COS-7 cells were transfected with ARNO siRNAs together with ARL4D(Q80L) or with ARL4D siRNA and FLAG-ARNO. Forty-eight hours after transfection, cells were fixed and stained with phalloidin to visualize F-actin and with anti-ARL4D or FLAG antibody to detect ARL4D(Q80L) and FLAG-ARNO. Cells transfected with each indicated construct to reduced stress fibers were assayed as described above. Error bars represent the SD of three independent experiments. *$p < 0.05$, calculated by *t* test and compared with ARL4D(Q80L) alone transfected cells. Bars, 10 μm.

with or without EGF (Figure 8, B and C). Quantitative fluorescence analyses confirm that ARNO redistribution to the plasma membrane by ARL4D was independent on PI3K activation (Figure 8C).

A previous report showed that a mutation (R279C) in the PH domain of ARNO abolishes PIP_3 binding and does not show EGF-stimulated translocation of the R279C mutant to the plasma membrane (Venkateswarlu and Cullen, 2000). Thus, we examined whether ARL4D could induce translocation of ARNO(R279C) to the plasma membrane (Figure 8, E–G). ARNO(R279C) was able to interact with ARL4D by yeast two-hybrid analysis (Figure 8D). Consistent with a previous report, ARNO(R279C) resides primarily in the cytosol (Figure 8E, left; Venkateswarlu and Cullen, 2000). When coexpressed with ARL4D(Q80L), we observed that ARNO(R279C) translocated to the plasma membrane (Figure 8E, right). Moreover, ARL4D-mediated redistribution of ARNO(R279C) to the plasma membrane was not blocked by wortmannin when cells were incubated with or without EGF (Figure 8, F and G). Collectively, these data suggested that ARL4D-mediated association of ARNO to the plasma membrane is dependent on interaction with plasma membrane-associated ARL4D, but not in a PIP_3-dependent manner.

ARL4D Recruits Other Members of Cytohesin Family, but Not Akt PH Domain, to the Plasma Membrane

Because of highly structural conservation of the PH domain in the cytohesin family (Ogasawara *et al.*, 2000), we next examined whether ARL4D can induce redistribution of other cyto-

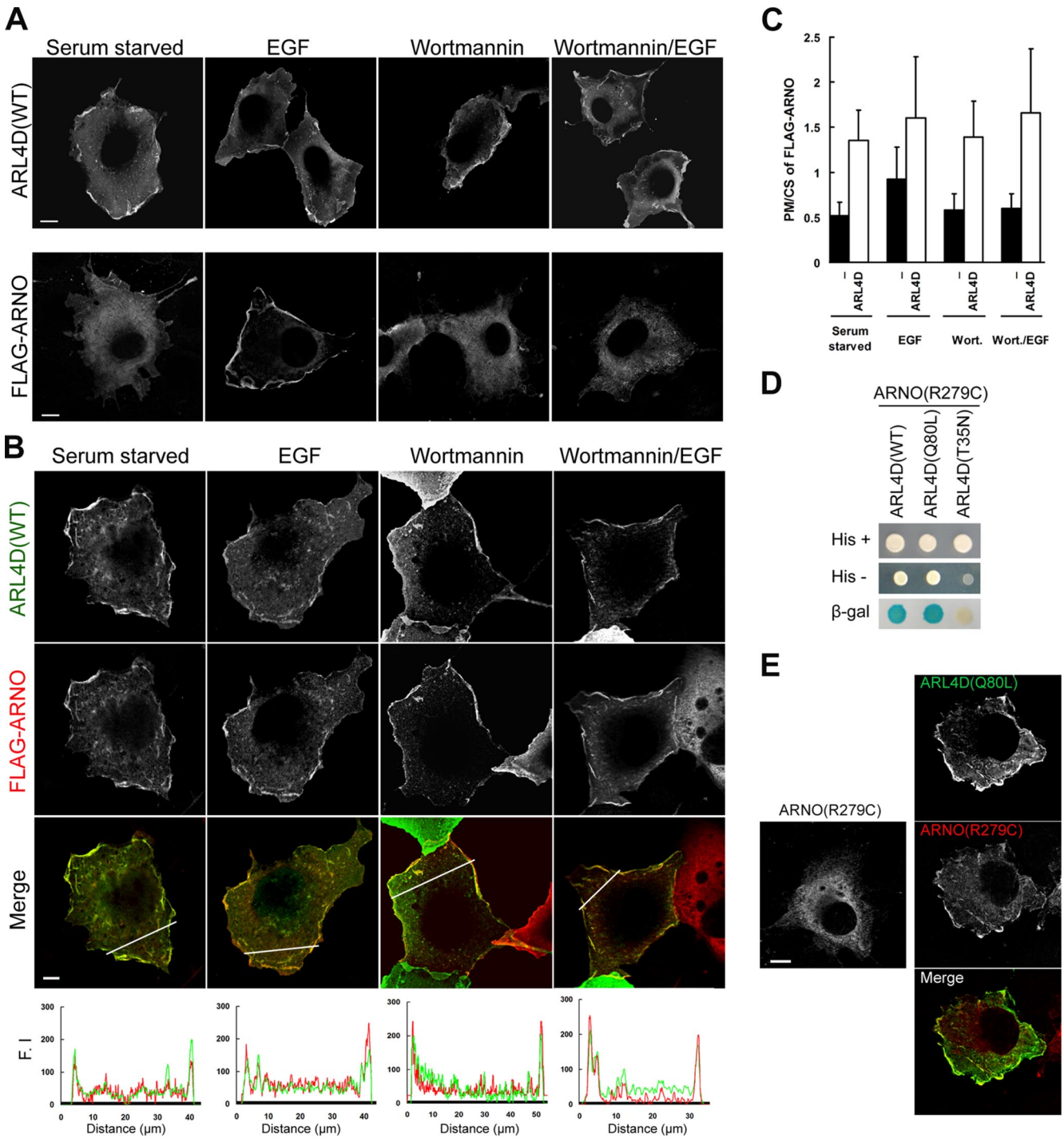

Figure 8. ARL4D-induced translocation of ARNO is not dependent on PI3K signaling. (A) Inhibitors of PI3K do not inhibit the plasma membrane localization of ARL4D. COS-7 cells transfected with ARL4D or FLAG-ARNO were serum starved, treated with EGF or wortmannin alone, or pretreated with wortmannin followed by EGF. The cells were then fixed immediately and stained with ARL4D or FLAG antibodies. (B) ARL4D recruitment of ARNO to the plasma membrane is PI3K independent. COS-7 cells cotransfected with ARL4D or FLAG-ARNO were examined as described above. (C) Quantification of ARNO localization in ARL4D-coexpressing cells as described in *Materials and Methods*. The fluorescence signals of ARNO were examine after EGF or wortmannin treatment from transfected FLAG-ARNO alone (black bar) or cotransfected with ARL4D (white bar) cells. At least 50 cells were analyzed for each condition from two separate experiments and error bars represent SD (D) ARL4D(Q80L) binds to ARNO(R279C) in yeast two-hybrid system. (E) ARL4D(Q80L) recruits ARNO(R279C) to the plasma membrane. COS-7 cells transfected with FLAG-ARNO(R279C) alone or cotransfected with ARL4(Q80L) were probed with antibodies against with ARL4D and FLAG. (F) ARNO(R279C), a PIP_3-binding abolished mutant, can be recruited to the plasma membrane by overexpressed ARL4D. COS-7 cells cotransfected with ARL4D or FLAG-ARNO(R279C) were examined as described above. (H) ARL4D did not recruit Akt-PH-GFP to the plasma membrane. COS-7 cells cotransfected with ARL4D and Akt-PH-GFP were examined as above. The membrane distribution of FLAG-ARNO(R279C) (G) and Akt-PH-GFP (I) were defined and quantified as per the methods used in Figure 4. More than 50 transfected cells were counted in each group. Data represent means ± SD of two independent experiments. Bar, 10 μm.

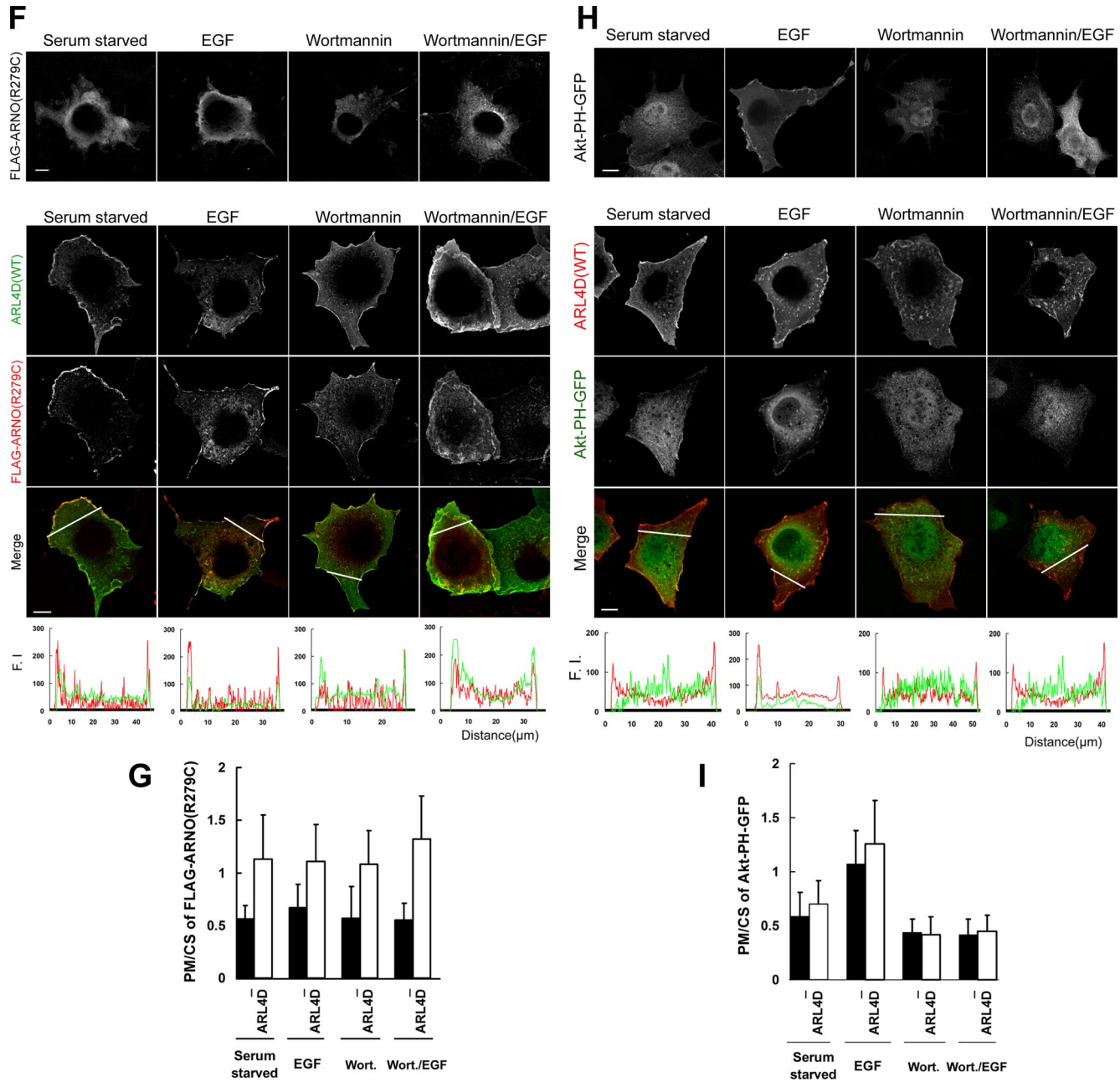

Figure 8. Continued.

hesins, including cytohesin-1, cytohesin-3, and cytohesin-4, to the plasma membrane. All FLAG-tagged cytohesins were diffusely localized throughout the cytoplasm (Supplemental Figure S7). When coexpressed with ARL4D(Q80L), the redistribution of FLAG-cytohesin-1, FLAG-cytohesin-3, and FLAG-cytohesin-4 to plasma membrane ruffles and protrusions was detected (Supplemental Figure S7). Together, these results illustrate that the effect of ARL4D on the subcellular localization of all members of the cytohesin family is similar.

Despite high primary sequence variability, PH domains retain a conserved three-dimensional organization consisting of seven-stranded β-sandwich structure, with one corner capped off by a C-terminal α-helix and another by three interstrand loops. However, different PH domains have different affinities to several kinds of phospholipids (Lemmon, 2004; Balla, 2005). There has been speculation about the key regulator(s) of their specificity (Lemmon, 2004; Balla, 2005; Varnai *et al.*, 2005), especially concerning the protein–protein interaction. Similar to the PH domain of ARNO, the PH domain of Akt showed growth-factor-stimulated and wortmannin-sensitive translocation from the cytosol to the plasma membrane (Gray *et al.*, 1999). Thus, we next examined whether ARL4D can induce translocation of Akt-PH-GFP to the plasma membrane. However, a yeast two-hybrid assay showed that ARL4D could not interact with Akt-PH (unpublished data). In control, Akt-PH-GFP is localized to the cytoplasm and the nucleus (Figure 8H, top). In EGF-stimulated cells with or without coexpressing ARL4D, we found that Akt-PH-GFP localized to the plasma membrane (Figure 8, H and I). However, unlike the effect on ARNO,

ARL4D did not induce redistribution of Akt-PH-GFP to the plasma membrane in the presence of wortmannin (Figure 8, H and I). This suggests that the interaction between ARL4D and cytohesin family proteins does not extend to another PIP3 membrane-associated PH domain-containing protein, and it reflects a novel and specific relationship between ARL4D and cytohesin family proteins.

DISCUSSION

In this study, we demonstrated that ARL4D could act as a novel upstream regulator of cytohesin-2/ARNO to modulate actin remodeling. Based on several lines of evidence, we suggest that ARL4D directly interacts with cytohesin-2/ARNO and recruits it to the plasma membrane in a PIP_3-independent manner to modulate actin remodeling. First, ARL4D bound to cytohesin-2/ARNO, and this interaction was dependent on the guanine-nucleotide bound by ARL4D and the C-terminal PH and polybasic c domains of ARNO. Second, localization of ARL4D at the plasma membrane was GTP- and N-terminal myristoylation dependent. Third, ARL4D induced translocation of ARNO to the plasma membrane and promoted activation of ARF6, resulting in the decrease of actin stress fibers. Fourth, siRNA-mediated down-regulation of ARL4D lead to a suppression in cell migration. Finally, ARL4D-induced translocation of cytohesin-2/ARNO to the plasma membrane did not require the activation of PI3K. We infer that ARL4D is activated by a yet to be identified signal to recruit cytohesin-2/ARNO to the plasma membrane, where ARNO activates ARF6 to induce actin reorganization (Figure 9).

Localization of ARL4D at the Plasma Membrane

Our previous studies showed that N-terminal EGFP- or C-terminal myc-tagged ARL4D was present in nuclei and partially in nucleoli, possibly through the interaction of its C-terminal bipartite NLS with importin-α (Lin *et al*., 2002; our unpublished data). In this study, we detected endogenous and nontagged recombinant ARL4D at the plasma membrane in addition to the nucleus and cytoplasm. This plasma membrane localization was GTP- and N-terminal myristoylation dependent. The differences in the intracellular distribution may result from the effects of epitope tags at either the N-terminal myristoylation site or near the C-terminal bipartite NLS, both of which are important for ARL4D localization. The staining of cells for endogenous ARL4D (Figure 3D) and overexpressed ARL4D (Figure 3A) is somewhat different. The staining pattern of overexpressed ARL4D seems to show less nuclear staining and more punctate cytosolic signals. Because the level of overexpressed ARL4D compared with the endogenous protein could be greater than 10-fold, increased overexpressed ARL4D protein might saturate nuclear sites or a nuclear import system, thereby increasing cytosolic signals. Recently, Barrios-Rodiles *et al*. (2005) showed that transforming growth factor-β signaling could stimulate interaction of ARL4D with Smad2 and subsequently recruit ARL4D to a Smad2/Smad4 complex. This observation indicates that ARL4D may play another role in the nucleus and/or nucleoli under specific signaling regulation.

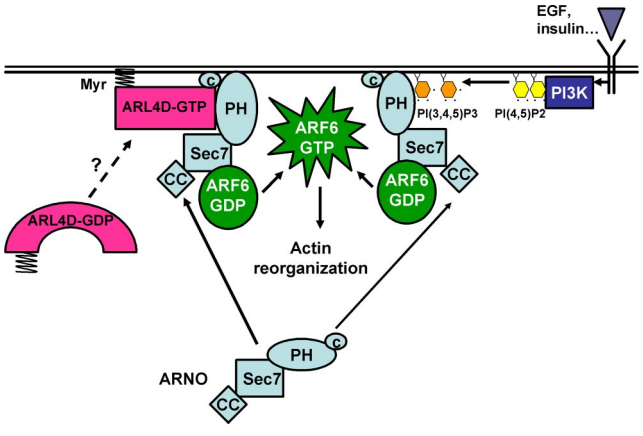

Figure 9. Model for the role of ARL4D in recruitment of ARNO and activation of ARF6. We speculate that ARL4D can be activated by an unidentified GEF. Through protein–protein interaction, the active form of ARL4D can recruit ARNO to the plasma membrane where ARNO efficiently activates ARF6. ARF6-GTP induces actin reorganization and membrane ruffling formation. ARL4D recruits ARNO to the plasma membrane through a PH domain and polybasic c domain-mediated interaction. The PI3K pathway is not involved in the regulation of ARL4D-mediated translocation of ARNO.

Cytohesin-2/ARNO Is a Downstream Effector of ARL4D

It is generally accepted that GEFs bind preferentially to GDP-bound or nucleotide-free GTPase, and GAPs to GTP-bound GTPase. The binary protein complex of nucleotide-free GTPase and GEF is thought to be an enzymatic reaction intermediate (Cherfils *et al*., 1998; Day *et al*., 1998). It is well established that ARNO stimulates nucleotide exchange on both ARF1 and ARF6 (Chardin *et al*., 1996; Frank *et al*., 1998a) through the Sec7 domain, with its hydrophobic surface groove for interaction with the switch 1 and switch 2 regions of ARFs (Betz *et al*., 1998; Goldberg, 1998; Mossessova *et al*., 1998; Pacheco-Rodriguez *et al*., 1999). ARNO-Sec7 formed a stable complex with the nucleotide-free form of NΔ17ARF1 (Paris *et al*., 1997; Beraud-Dufour *et al*., 1998). Unlike the typical association of a GEF with its substrate, an association between ARL4D and ARNO was found with ARL4D is in a GTP-bound state. This observation contrasts sharply with findings for the association between GEF and its bona fide substrates. The binding site for ARL4D(Q80L) in ARNO lies in the C-terminal PH domain and polybasic c domain, but not the Sec7 domain, indicating that ARNO may serve as an ARL effector rather than an activator. Moreover, our data showed that ARNO is not a GEF for ARL4D. Consistent with this notion, we showed that ARNO and ARNO(E156K) were translocated to the plasma membrane when they were coexpressed with ARL4D(Q80L). In addition, the amount of ARNO localized at the plasma membrane was not altered in cells coexpressing the membrane localization-defective mutant, ARL4D(G2A), although ARL4D(G2A) interacted with ARNO. We suggest that ARL4D might directly serve as a determinant for ARNO targeting to the plasma membrane.

ARL4D Modulates Actin Remodeling via Regulating ARNO and ARF6 Activity

In cells overexpressing ARL4D or ARL4D(Q80L), we observed a paucity of actin stress fibers. The effects of ARL4D on the actin cytoskeleton depend on its localization and the guanine nucleotide-bound state. Mutants with decreased affinity for GTP (T35N) or unable to localize at the plasma membrane (lacking the myristorylation site [G2A]) are unable to modulate actin remodeling.

ARF6-GTP initiates cortical actin rearrangement at the cell periphery, accompanied by a depletion of stress fibers (D'Souza-Schorey *et al*., 1997; Boshans *et al*., 2000). Previous

studies had indicated that ARNO might be the GEF for ARF6. Overexpression of ARNO lead to disassembly of actin stress fibers, remodeling of the cortical actin cytoskeleton in HeLa cells (Frank *et al*., 1998b), and development of broad lamellipodia in MDCK cells with a dramatic increase in migratory behavior (Santy and Casanova, 2001). Coexpression of ARF6(T27N) or ARNO(E156K), or depletion of ARNO content with siRNA, prevented ARL4D(Q80L)-induced actin disassembly, suggesting that the activation of ARF6 and ARNO are downstream effects of ARL4D. ARNO-induced actin reorganization did not differ significantly in cells with reduced ARL4D expression, further supporting the idea. However, the amounts of actin stress fibers in ARNO-depleted cells overexpressing ARL4D(Q80L) were not as high as those cells overexpressing ARL4D(T35N) or inactive ARNO. Perhaps the action of ARNO remaining in siRNA-treated cells or of the other similar cytohesin/ARNO proteins may account for only partial decrease of actin stress fibers.

The overexpression of ARNO or activation of ARF6 induced a migratory phenotype (Palacios *et al*., 2001; Santy and Casanova, 2001). It was also reported that expression of ARNO(E156K), which cannot activate ARF6, caused a decrease in cell mobility (Santy and Casanova, 2001), and suppression of ARF6 blocked invasive and migration activities of breast cancer cells (Hashimoto *et al*., 2004). This is consistent with our finding of reduced cell mobility in ARL4D siRNA knockdown cells. Our results are consistent with the notion that ARL4D increases activation of ARF6 by recruiting ARNO to the plasma membrane, followed by reorganization of the actin cytoskeleton and enhanced cell migration.

Some Ras superfamily GTPases have been shown to regulate each another via modulated GEF activities. Ras activated Ral through the direct association with the Ral-GEF RalGDS (Feig, 2003) and activated Rac by stimulating the activity of the Rac1-specific GEF Tiam1 (Lambert *et al*., 2002). In *Schizosaccharomyces pombe*, GTP-Ras interacted with Scd1, a RhoGEF, to promote Cdc42 activation (Chang *et al*., 1994). To our knowledge, this is the first report describing the coordination of GTPase cascade through an ARF-GEF.

ARL4D-induced Translocation of ARNO via the PH Domain Is Independent of PI3-Kinase Signaling

PH domains are well-known for their ability specifically to bind phosphoinositides for cellular membrane targeting of proteins. Membrane targeting of PH-containing protein is often important for functional activation in precise spatial and temporal regulation. The PH domain of the cytohesin family proteins is necessary for membrane association, PIP_3 binding, and recruitment to the plasma membrane of cells stimulated with growth factor in a PI3K-dependent manner (Klarlund *et al*., 1997; Nagel *et al*., 1998b; Venkateswarlu *et al*., 1998; Klarlund *et al*., 2000). Our data provide a new mechanism for regulation of ARNO by protein–protein interaction. ARL4D overexpression facilitated ARNO translocation to the plasma membrane even in the presence of PI3K inhibitor, and PIP_3-binding defective mutant ARNO(R279C) could still be recruited to the plasma membrane upon ARL4D overexpression. ARL4D did not interact with PH domain from Akt, proving that its interaction with cytohesin family PH domain is specific. Several PH domain-containing proteins are reported to interact via their PH domains with small GTPases (Lemmon, 2004). The PH domain of FAPP1 bound directly to ARF1 and targets it to Golgi (Godi *et al*., 2004) and that of PLC-β2 acted as an effector site for Rac (Snyder *et al*., 2003), whereas RhoA bound to the N-terminal PH domain of the Btk family tyrosine kinase Etk (Kim *et al*., 2002). Our findings that ARL4D can interact via PH domains of cytohesin family proteins are in agreement with these results. We also showed that ARL4A and ARL4C recruited ARNO/cytohesin2 to the plasma membrane (Supplemental Figure S8). While this manuscript was under revision, Munro and colleagues (Hofmann *et al*., 2007; published online ahead of print on March 28, 2007, in the Current Biology) reported that the ARL4 family of small G proteins could recruit the cytohesin ARF6 exchange factors to the plasma membrane, consistent with our results. Although the ARL4 family can interact with all cytohesin members, the differential expression of ARL4s and cytohesins in different tissues and during different stages of development (Schurmann *et al*., 1994; Jacobs *et al*., 1999; Lin *et al*., 2000, 2002; Ogasawara *et al*., 2000) provides a means to regulate the elaborate signaling pathway in eukaryotes. Interestingly, Donaldson and colleagues (Cohen *et al*., 2007; published online ahead of print on April 4, 2007, in the Mol. Biol. Cell) showed that ARF6 could also bind to the PH domain of ARNO and recruit it to the plasma membrane. Therefore, it is plausible that recruitment of ARNO family GEFs to the plasma membrane for further activation of other ARF isoforms might be dependent on differential expression of ARL4s and ARF6 in different cell types.

The precise subcellular localization of GTPase activation is required for the proper initiation of downstream signaling events. The biochemical mechanism upstream of ARL4D-mediated regulation of ARNO signaling is not known yet. Knowing that the expression of ARL4A and ARL4D are developmentally regulated and tissue specific (Lin *et al*., 2000, 2002), and that ARNO can regulate dendritic development (Hernandez-Deviez *et al*., 2002), it will be important to define precisely the signaling events upstream of ARL4 activation and their functional consequences during development.

ACKNOWLEDGMENTS

We thank Drs. Randy Haun (University of Arkansas for Medical Sciences, Little Rock, AR), Martha Vaughan (National Institutes of Health), and Chun-Fang Huang for critical review of this manuscript. Experiments and image analysis were performed in part through the use of the Cell Imaging Center (Core lab 2) at National Taiwan University Hospital and with the assistance of Shu-Chen Shen. We also thank laboratory members at Core lab 6 (especially to Shu-Tieng You, Yueh-Tso Tsai, and Yi-Jiun Chen) for help purifying recombinant proteins. This work was supported by grants from the National Science Council, R.O.C. (NSC 91GMP032-2, NSC 95GMP032-2, NSC 96-2752-B-002-007-PAE), National Taiwan University Hospital (94A12-1, 95A12-1, 96A12-1), and the Yung-Shin Biomedical Research Funds (YSP-86-019) to F.-J.S.L. This research was supported in part by the Intramural Research Program, National Heart, Lung, and Blood Institute, National Institutes of Health.

REFERENCES

Balch, W. E., Kahn, R. A., and Schwaninger, R. (1992). ADP-ribosylation factor is required for vesicular trafficking between the endoplasmic reticulum and the cis-Golgi compartment. J. Biol. Chem. *267*, 13053–13061.

Balla, T. (2005). Inositol-lipid binding motifs: signal integrators through protein-lipid and protein-protein interactions. J. Cell Sci. *118*, 2093–2104.

Barrios-Rodiles, M. *et al*. (2005). High-throughput mapping of a dynamic signaling network in mammalian cells. Science *307*, 1621–1625.

Beraud-Dufour, S., Robineau, S., Chardin, P., Paris, S., Chabre, M., Cherfils, J., and Antonny, B. (1998). A glutamic finger in the guanine nucleotide exchange factor ARNO displaces Mg2+ and the beta-phosphate to destabilize GDP on ARF1. EMBO J. *17*, 3651–3659.

Betz, S. F. *et al*. (1998). Solution structure of the cytohesin-1 (B2–1) Sec7 domain and its interaction with the GTPase ADP ribosylation factor 1. Proc. Natl. Acad. Sci. USA *95*, 7909–7914.

Bhamidipati, A., Lewis, S. A., and Cowan, N. J. (2000). ADP ribosylation factor-like protein 2 (Arl2) regulates the interaction of tubulin-folding cofactor D with native tubulin. J. Cell Biol. *149*, 1087–1096.

Boshans, R. L., Szanto, S., van Aelst, L., and D'Souza-Schorey, C. (2000). ADP-ribosylation factor 6 regulates actin cytoskeleton remodeling in coordination with Rac1 and RhoA. Mol. Cell Biol. *20*, 3685–3694.

Burd, C. G., Strochlic, T. I., and Gangi Setty, S. R. (2004). Arf-like GTPases: not so Arf-like after all. Trends Cell Biol. *14*, 687–694.

Chang, E. C., Barr, M., Wang, Y., Jung, V., Xu, H. P., and Wigler, M. H. (1994). Cooperative interaction of *S. pombe* proteins required for mating and morphogenesis. Cell *79*, 131–141.

Chardin, P., Paris, S., Antonny, B., Robineau, S., Beraud-Dufour, S., Jackson, C. L., and Chabre, M. (1996). A human exchange factor for ARF contains Sec7- and pleckstrin-homology domains. Nature *384*, 481–484.

Chavrier, P., and Goud, B. (1999). The role of ARF and Rab GTPases in membrane transport. Curr. Opin. Cell Biol. *11*, 466–475.

Cherfils, J., Menetrey, J., Mathieu, M., Le Bras, G., Robineau, S., Beraud-Dufour, S., Antonny, B., and Chardin, P. (1998). Structure of the Sec7 domain of the Arf exchange factor ARNO. Nature *392*, 101–105.

Cohen, L. A., Honda, A., Varnai, P., Brown, F. D., Balla, T., and Donaldson. J. G. (2007). Active Arf6 recruits ARNO/cytohesin GEFs to the PM by binding their PH domains. Mol. Biol. Cell *18*, 2244–2253.

Cullen, P. J., and Chardin, P. (2000). Membrane targeting: what a difference a G makes. Curr. Biol. *10*, R876–R878.

D'Souza-Schorey, C., Boshans, R. L., McDonough, M., Stahl, P. D., and Van Aelst, L. (1997). A role for POR1, a Rac1-interacting protein, in ARF6-mediated cytoskeletal rearrangements. EMBO J. *16*, 5445–5454.

D'Souza-Schorey, C., and Chavrier, P. (2006). ARF proteins: roles in membrane traffic and beyond. Nat. Rev. Mol. Cell Biol. *7*, 347–358.

D'Souza-Schorey, C., Li, G., Colombo, M. I., and Stahl, P. D. (1995). A regulatory role for ARF6 in receptor-mediated endocytosis. Science *267*, 1175–1178.

Day, G. J., Mosteller, R. D., and Broek, D. (1998). Distinct subclasses of small GTPases interact with guanine nucleotide exchange factors in a similar manner. Mol. Cell Biol. *18*, 7444–7454.

Dierks, H., Kolanus, J., and Kolanus, W. (2001). Actin cytoskeletal association of cytohesin-1 is regulated by specific phosphorylation of its carboxyl-terminal polybasic domain. J. Biol. Chem. *276*, 37472–37481.

Donaldson, J. G. (2003). Multiple roles for Arf 6, sorting, structuring, and signaling at the plasma membrane. J. Biol. Chem. *278*, 41573–41576.

Donaldson, J. G., and Jackson, C. L. (2000). Regulators and effectors of the ARF GTPases. Curr. Opin. Cell Biol. *12*, 475–482.

Feig, L. A. (2003). Ral-GTPases: approaching their 15 minutes of fame. Trends Cell Biol. *13*, 419–425.

Fournier, H. N., Dupe-Manet, S., Bouvard, D., Luton, F., Degani, S., Block, M. R., Retta, S. F., and Albiges-Rizo, C. (2005). Nuclear translocation of integrin cytoplasmic domain-associated protein 1 stimulates cellular proliferation. Mol. Biol. Cell *16*, 1859–1871.

Franco, M., Peters, P. J., Boretto, J., van Donselaar, E., Neri, A., D'Souza-Schorey, C., and Chavrier, P. (1999). EFA6, a sec7 domain-containing exchange factor for ARF6, coordinates membrane recycling and actin cytoskeleton organization. EMBO J. *18*, 1480–1491.

Frank, S., Upender, S., Hansen, S. H., and Casanova, J. E. (1998a). ARNO is a guanine nucleotide exchange factor for ADP-ribosylation factor 6. J. Biol. Chem. *273*, 23–27.

Frank, S. R., Hatfield, J. C., and Casanova, J. E. (1998b). Remodeling of the actin cytoskeleton is coordinately regulated by protein kinase C and the ADP-ribosylation factor nucleotide exchange factor ARNO. Mol. Biol. Cell *9*, 3133–3146.

Godi, A., Di Campli, A., Konstantakopoulos, A., Di Tullio, G., Alessi, D. R., Kular, G. S., Daniele, T., Marra, P., Lucocq, J. M., and De Matteis, M. A. (2004). FAPPs control Golgi-to-cell-surface membrane traffic by binding to ARF and PtdIns(4)P. Nat. Cell Biol. *6*, 393–404.

Goldberg, J. (1998). Structural basis for activation of ARF GTPase: mechanisms of guanine nucleotide exchange and GTP-myristoyl switching. Cell *95*, 237–248.

Gray, A., Van Der Kaay, J., and Downes, C. P. (1999). The pleckstrin homology domains of protein kinase B and GRP1 (general receptor for phosphoinositides-1) are sensitive and selective probes for the cellular detection of phosphatidylinositol 3,4-bisphosphate and/or phosphatidylinositol 3,4,5-trisphosphate in vivo. Biochem. J. *344*, 929–936.

Harshman, K. *et al.* (1995). Comparison of the positional cloning methods used to isolate the BRCA1 gene. Hum. Mol. Genet. *4*, 1259–1266.

Hashimoto, S., Onodera, Y., Hashimoto, A., Tanaka, M., Hamaguchi, M., Yamada, A., and Sabe, H. (2004). Requirement for Arf6 in breast cancer invasive activities. Proc. Natl. Acad. Sci. USA *101*, 6647–6652.

Hemmings, B. A. (1997). PH domains–a universal membrane adapter. Science *275*, 1899

Hernandez-Deviez, D. J., Casanova, J. E., and Wilson, J. M. (2002). Regulation of dendritic development by the ARF exchange factor ARNO. Nat. Neurosci. *5*, 623–624.

Hofmann, I., Thompson, A., Sanderson, C. M., and Munro, S. (2007). The Arl4 family of small G proteins can recruit the cytohesin Arf6 exchange factors to the plasma membrane. Curr. Biol. *17*, 711–716.

Jackson, C. L., and Casanova, J. E. (2000). Turning on ARF: the Sec7 family of guanine-nucleotide-exchange factors. Trends Cell Biol. *10*, 60–67.

Jackson, T. R., Kearns, B. G., and Theibert, A. B. (2000). Cytohesins and centaurins: mediators of PI 3-kinase-regulated Arf signaling. Trends Biochem. Sci. *25*, 489–495.

Jacobs, S., Schilf, C., Fliegert, F., Koling, S., Weber, Y., Schurmann, A., and Joost, H. G. (1999). ADP-ribosylation factor (ARF)-like 4, 6, and 7 represent a subgroup of the ARF family characterization by rapid nucleotide exchange and a nuclear localization signal. FEBS Lett. *456*, 384–388.

Kahn, R. A., Cherfils, J., Elias, M., Lovering, R. C., Munro, S., and Schurmann, A. (2006). Nomenclature for the human Arf family of GTP-binding proteins: ARF, ARL, and SAR proteins. J. Cell Biol. *172*, 645–650.

Kim, O., Yang, J., and Qiu, Y. (2002). Selective activation of small GTPase RhoA by tyrosine kinase Etk through its pleckstrin homology domain. J. Biol. Chem. *277*, 30066–30071.

Klarlund, J. K., Guilherme, A., Holik, J. J., Virbasius, J. V., Chawla, A., and Czech, M. P. (1997). Signaling by phosphoinositide-3,4,5-trisphosphate through proteins containing pleckstrin and Sec7 homology domains. Science *275*, 1927–1930.

Klarlund, J. K., Tsiaras, W., Holik, J. J., Chawla, A., and Czech, M. P. (2000). Distinct polyphosphoinositide binding selectivities for pleckstrin homology domains of GRP1-like proteins based on diglycine versus triglycine motifs. J. Biol. Chem. *275*, 32816–32821.

Kremer, W., Steiner, G., Beraud-Dufour, S., and Kalbitzer, H. R. (2004). Conformational states of the small G protein Arf-1 in complex with the guanine nucleotide exchange factor ARNO-Sec7. J. Biol. Chem. *279*, 17004–17012.

Laemmli, U. K. (1970). Cleavage of structural proteins during the assembly of the head of bacteriophage T4. Nature *227*, 680–685.

Lambert, J. M., Lambert, Q. T., Reuther, G. W., Malliri, A., Siderovski, D. P., Sondek, J., Collard, J. G., and Der, C. J. (2002). Tiam1 mediates Ras activation of Rac by a PI(3)K-independent mechanism. Nat. Cell Biol. *4*, 621–625.

Lemmon, M. A. (2004). Pleckstrin homology domains: not just for phosphoinositides. Biochem. Soc. Trans. *32*, 707–711.

Lin, C. Y., Huang, P. H., Liao, W. L., Cheng, H. J., Huang, C. F., Kuo, J. C., Patton, W. A., Massenburg, D., Moss, J., and Lee, F. J. (2000). ARL4, an ARF-like protein that is developmentally regulated and localized to nuclei and nucleoli. J. Biol. Chem. *275*, 37815–37823.

Lin, C. Y., Li, C. C., Huang, P. H., and Lee, F. J. (2002). A developmentally regulated ARF-like 5 protein (ARL5), localized to nuclei and nucleoli, interacts with heterochromatin protein 1. J. Cell Sci. *115*, 4433–4445.

Lu, L., Tai, G., and Hong, W. (2004). Autoantigen Golgin-97, an effector of Arl1 GTPase, participates in traffic from the endosome to the trans-Golgi network. Mol. Biol. Cell *15*, 4426–4443.

Macia, E., Paris, S., and Chabre, M. (2000). Binding of the PH and polybasic C-terminal domains of ARNO to phosphoinositides and to acidic lipids. Biochemistry *39*, 5893–5901.

Mansour, M., Lee, S. Y., and Pohajdak, B. (2002). The N-terminal coiled coil domain of the cytohesin/ARNO family of guanine nucleotide exchange factors interacts with the scaffolding protein CASP. J. Biol. Chem. *277*, 32302–32309.

Moss, J., and Vaughan, M. (1998). Molecules in the ARF orbit. J. Biol. Chem. *273*, 21431–21434.

Moss, J., and Vaughan, M. (2002). Cytohesin-1 in 2001. Arch. Biochem. Biophys. *397*, 156–161.

Mossessova, E., Gulbis, J. M., and Goldberg, J. (1998). Structure of the guanine nucleotide exchange factor Sec7 domain of human arno and analysis of the interaction with ARF GTPase. Cell *92*, 415–423.

Nagel, W., Schilcher, P., Zeitlmann, L., and Kolanus, W. (1998a). The PH domain and the polybasic c domain of cytohesin-1 cooperate specifically in

plasma membrane association and cellular function. Mol. Biol. Cell *9*, 1981–1994.

Nagel, W., Zeitlmann, L., Schilcher, P., Geiger, C., Kolanus, J., and Kolanus, W. (1998b). Phosphoinositide 3-OH kinase activates the beta2 integrin adhesion pathway and induces membrane recruitment of cytohesin-1. J. Biol. Chem. *273*, 14853–14861.

Ogasawara, M., Kim, S. C., Adamik, R., Togawa, A., Ferrans, V. J., Takeda, K., Kirby, M., Moss, J., and Vaughan, M. (2000). Similarities in function and gene structure of cytohesin-4 and cytohesin-1, guanine nucleotide-exchange proteins for ADP-ribosylation factors. J. Biol. Chem. *275*, 3221–3230.

Pacheco-Rodriguez, G., Meacci, E., Vitale, N., Moss, J., and Vaughan, M. (1998). Guanine nucleotide exchange on ADP-ribosylation factors catalyzed by cytohesin-1 and its Sec7 domain. J. Biol. Chem. *273*, 26543–26548.

Pacheco-Rodriguez, G., Patton, W. A., Adamik, R., Yoo, H. S., Lee, F. J., Zhang, G. F., Moss, J., and Vaughan, M. (1999). Structural elements of ADP-ribosylation factor 1 required for functional interaction with cytohesin-1. J. Biol. Chem. *274*, 12438–12444.

Palacios, F., Price, L., Schweitzer, J., Collard, J. G., and D'Souza-Schorey, C. (2001). An essential role for ARF6-regulated membrane traffic in adherens junction turnover and epithelial cell migration. EMBO J. *20*, 4973–4986.

Paris, S., Beraud-Dufour, S., Robineau, S., Bigay, J., Antonny, B., Chabre, M., and Chardin, P. (1997). Role of protein-phospholipid interactions in the activation of ARF1 by the guanine nucleotide exchange factor Arno. J. Biol. Chem. *272*, 22221–22226.

Poupel, O., Boleti, H., Axisa, S., Couture-Tosi, E., and Tardieux, I. (2000). Toxofilin, a novel actin-binding protein from Toxoplasma gondii, sequesters actin monomers and caps actin filaments. Mol. Biol. Cell *11*, 355–368.

Radhakrishna, H., and Donaldson, J. G. (1997). ADP-ribosylation factor 6 regulates a novel plasma membrane recycling pathway. J. Cell Biol. *139*, 49–61.

Radhakrishna, H., Klausner, R. D., and Donaldson, J. G. (1996). Aluminum fluoride stimulates surface protrusions in cells overexpressing the ARF6 GTPase. J. Cell Biol. *134*, 935–947.

Sabe, H. (2003). Requirement for Arf6 in cell adhesion, migration, and cancer cell invasion. J. Biochem. *134*, 485–489.

Santy, L. C., and Casanova, J. E. (2001). Activation of ARF6 by ARNO stimulates epithelial cell migration through downstream activation of both Rac1 and phospholipase D. J. Cell Biol. *154*, 599–610.

Santy, L. C., Frank, S. R., Hatfield, J. C., and Casanova, J. E. (1999). Regulation of ARNO nucleotide exchange by a PH domain electrostatic switch. Curr. Biol. *9*, 1173–1176.

Schurmann, A., Breiner, M., Becker, W., Huppertz, C., Kainulainen, H., Kentrup, H., and Joost, H. G. (1994). Cloning of two novel ADP-ribosylation factor-like proteins and characterization of their differential expression in 3T3–L1 cells. J. Biol. Chem. *269*, 15683–15688.

Schurmann, A., Koling, S., Jacobs, S., Saftig, P., Krauss, S., Wennemuth, G., Kluge, R., and Joost, H. G. (2002). Reduced sperm count and normal fertility in male mice with targeted disruption of the ADP-ribosylation factor-like 4 (Arl4) gene. Mol. Cell Biol. *22*, 2761–2768.

Shin, H. W., and Nakayama, K. (2004). Guanine nucleotide-exchange factors for arf GTPases: their diverse functions in membrane traffic. J. Biochem. *136*, 761–767.

Smith, S. A., Holik, P. R., Stevens, J., Melis, R., White, R., and Albertsen, H. (1995). Isolation and mapping of a gene encoding a novel human ADP-ribosylation factor on chromosome 17q12–q21. Genomics *28*, 113–115.

Snyder, J. T., Singer, A. U., Wing, M. R., Harden, T. K., and Sondek, J. (2003). The pleckstrin homology domain of phospholipase C-beta2 as an effector site for Rac. J. Biol. Chem. *278*, 21099–21104.

Stearns, T., Willingham, M. C., Botstein, D., and Kahn, R. A. (1990). ADP-ribosylation factor is functionally and physically associated with the Golgi complex. Proc. Natl. Acad. Sci. USA *87*, 1238–1242.

Takai, Y., Sasaki, T., and Matozaki, T. (2001). Small GTP-binding proteins. Physiol. Rev. *81*, 153–208.

Ueda, H., Fujita, R., Yoshida, A., Matsunaga, H., and Ueda, M. (2007). Identification of prothymosin-alpha1, the necrosis-apoptosis switch molecule in cortical neuronal cultures. J. Cell Biol. *176*, 853–862.

Varnai, P., Bondeva, T., Tamas, P., Toth, B., Buday, L., Hunyady, L., and Balla, T. (2005). Selective cellular effects of overexpressed pleckstrin-homology domains that recognize PtdIns(3,4,5)P3 suggest their interaction with protein binding partners. J. Cell Sci. *118*, 4879–4888.

Venkateswarlu, K. (2003). Interaction protein for cytohesin exchange factors 1 (IPCEF1) binds cytohesin 2 and modifies its activity. J. Biol. Chem. *278*, 43460–43469.

Venkateswarlu, K., and Cullen, P. J. (2000). Signalling via ADP-ribosylation factor 6 lies downstream of phosphatidylinositide 3-kinase. Biochem. J. *345*, 719–724.

Venkateswarlu, K., Gunn-Moore, F., Tavare, J. M., and Cullen, P. J. (1999). EGF-and NGF-stimulated translocation of cytohesin-1 to the plasma membrane of PC12 cells requires PI 3-kinase activation and a functional cytohesin-1 PH domain. J. Cell Sci. *112*, 1957–1965.

Venkateswarlu, K., Oatey, P. B., Tavare, J. M., and Cullen, P. J. (1998). Insulin-dependent translocation of ARNO to the plasma membrane of adipocytes requires phosphatidylinositol 3-kinase. Curr. Biol. *8*, 463–466.

Yamashiro, S., Chern, H., Yamakita, Y., and Matsumura, F. (2001). Mutant Caldesmon lacking cdc2 phosphorylation sites delays M-phase entry and inhibits cytokinesis. Mol. Biol. Cell *12*, 239–250.